Materials Characterization at Nano Scale: Importance and Implications

Avanish Kumar Srivastava

National Physical Laboratory
(Council of Scientific and Industrial Research)
New Delhi 110 012, INDIA

May 05, 2012

Seminar on Nano Technology
The Indian Institute of Metals
Delhi Chapter

Main Research Work

Growth, microstructure and properties evaluation of various metals & alloys and semiconducting nanostructures

Nucleation-growth mechanisms and phase transformations

In-situ image – spectrum interpretations

Various oxide nanostructures and phase formations

Evolution of optical bands and mechanical properties depending nano-scaled morphologies

Safe use of nanomaterials

Internal / External research projects in NPL

(NWP, MNES, DST, CSIR, DST-NSF, DST-JSPS)

- Study of droplet dynamics and heat flow characteristics during spray atomization and deposition
- Bulk Aluminum alloy – nSiC nano-composites
- Metal-induced crystallization of amorphous Si thin films
- Physico-chemical studies of metal and metal oxide Nanoparticles
- Development of Nano-structured Porous Materials
- Synthesis of Nanophase Luminiscent Materials & Devices
- Nanotubes of Carbon and Boron nitride
- Growth and characterization of Gold nano-particles as CRM
- Study of defect centres in nanomaterials for applications in sensors
- Custom Tailored Special Materials
- Establishment of high resolution TEM facility at NPL as an important part of Centre for Nanoscale Science

Future Research Projects ....

- Development of thermoelectric SiGe bulk nanocomposites with enhanced figure-of-merit for high temperature applications
- Pinning of flux lines by magnetic nanoparticles in high kappa superconductors
- Spintronics: Exploring Graphene
- Establishment of EELS to a new high resolution TEM facility

Significant contribution in the field of metal sciences and nanomaterials:

Grain microstructure, interface studies and phase formations in rapidly solidified and mechanically processed systems

Revelation of Multilayered thin films including spectroscopic evaluations on different topics: (i) Metal induced crystallization of amorphous Si and (ii) Al-Mn alloys multilayered thin films

Shape-selective growth, microstructure, spectroscopic and optical & mechanical response of bare & doped ZnO, CuO and Al_2O_3 nanostructures

Electron microscopy investigations on tungsten oxide, PEDOT and composite films with a novel microstructure for fast switching smart windows

Dynamics of Polymorphic Antimony Nanostructures: From Growth to Collapse, experimental and theoretical interpretations

A facile and novel synthesis of Ag-graphene based nanocomposites

Revelation of graphene-Au nano-composites for direct write deposition and electrical performance

Microstructure v/s Nanostructure

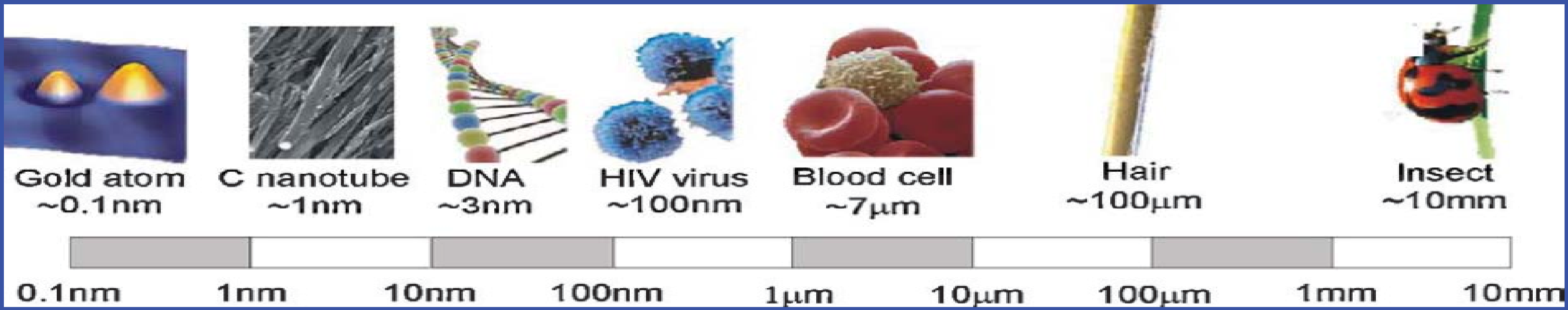

	Microstructure / Bulk	Nanostructure
Physics	Semi-classical	Quantum mechanical
Electron's nature	Particle-like	Wave-like
E or k-space	Continuous	Discrete
Current	Continuous	Quantized
Decision	Deterministic	Probabilistic
Fabrication	Micro-fabrication	Nano-fabrication
Surface to volume ratio	Small	Very large
Packing	Low	Very high

Carbon Nanotubes

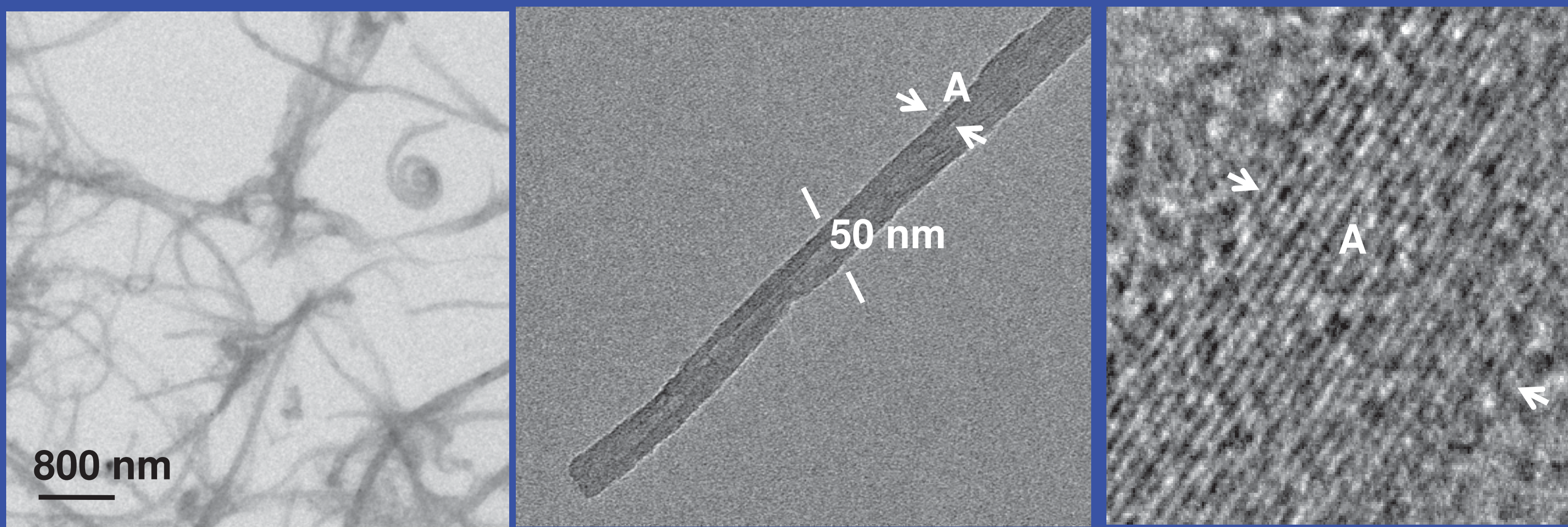

Boron Nitride Nanotubes

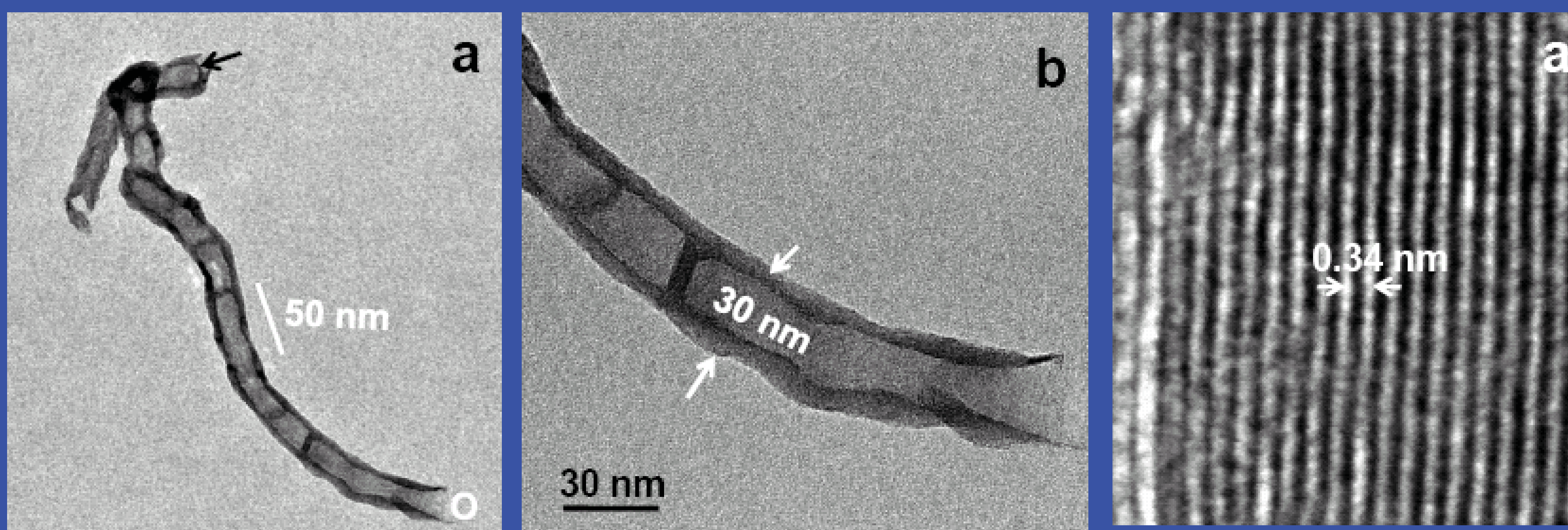

Nano-materials

Metals
Semiconductors
Insulators
Superconductors
magnetic materials

Oxides
Sulfides
Nitrides
Carbon

Methods for Synthesis of Nanomaterials

- **Physical**
  - **Mechanical**
    - High energy ball Milling, melt mixing
  - **Vapor**
    - Physical vapor deposition
    - Laser ablation, Sputter deposition, Electric arc deposition
    - Ion implantation
- **Chemical**
  - Colloids, sol-gels, L-B films, Inverse micelles
- **Biological**
  - Using biomembranes, DNA, enzymes and micro organisms
- **Hybrid**
  - Electrochemical, Chemical vapor deposition, Particle arresting in glass or zeolites or polymers, Micro emulsion

Techniques for Materials Characterization

Scanning Electron Microscopy

Scanning Tunneling Microscopy, Atomic Force Microscopy

Transmission Electron Microscopy

Energy-Dispersive X-Ray Spectroscopy

Electron Energy-Loss Spectroscopy

Scanning Transmission Electron Microscopy

X-Ray Diffraction

X-Ray Photoelectron Spectroscopy

Auger Electron Spectroscopy

X-Ray Fluorescence

Fourier Transform Infrared Spectroscopy

Raman Spectroscopy

Secondary Ion Mass Spectrometry

Electron Paramagnetic Resonance

Cathodoluminescence

Photoluminescence

Solidification Morphology

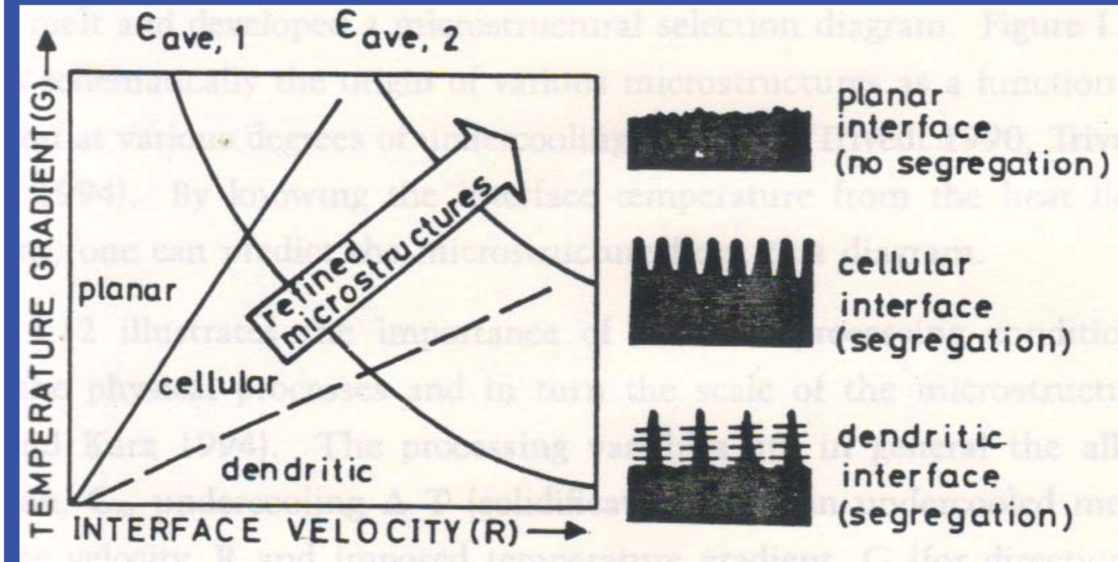

Dependence of solidification morphology on temperature gradient G & interface velocity R, qualitative effect of increasing average cooling rate εave = GR is indicated by sloping arrow (Mehrabian1982)

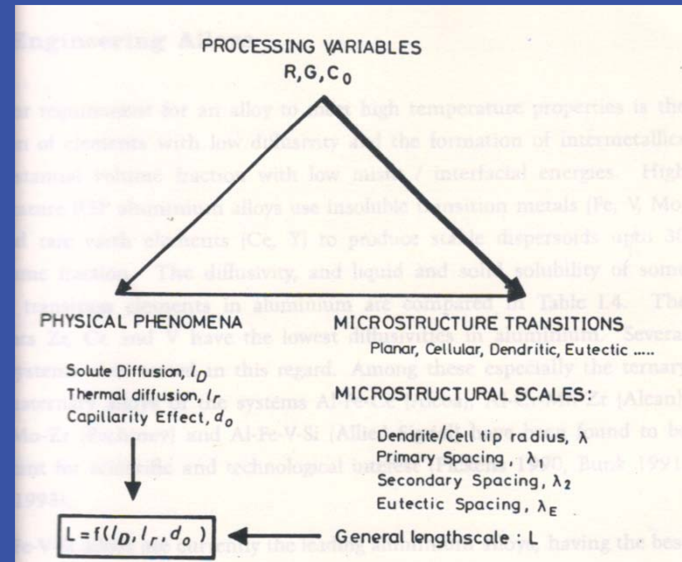

Correlation between processing variables & microstructure length scales, characteristic lengths of physical processes (Trivedi, Kurz 1994)

Crystal structure and Microstructure

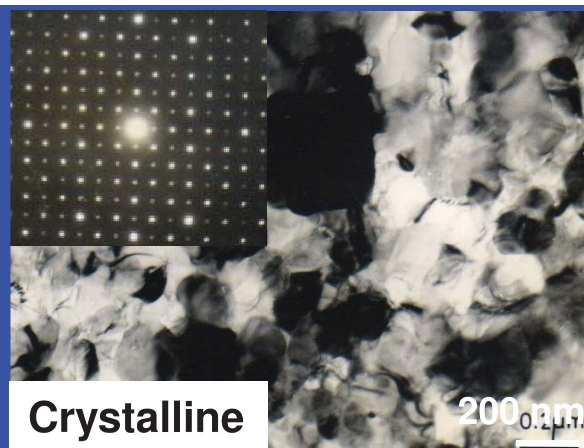

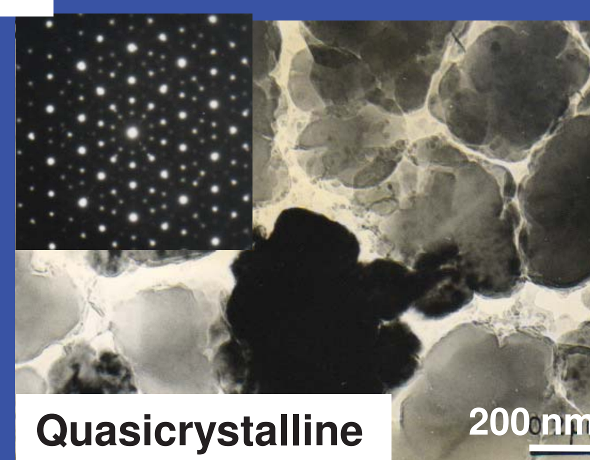

Quasicrystals and related crystals in Al-Mn and Al-Fe based alloys

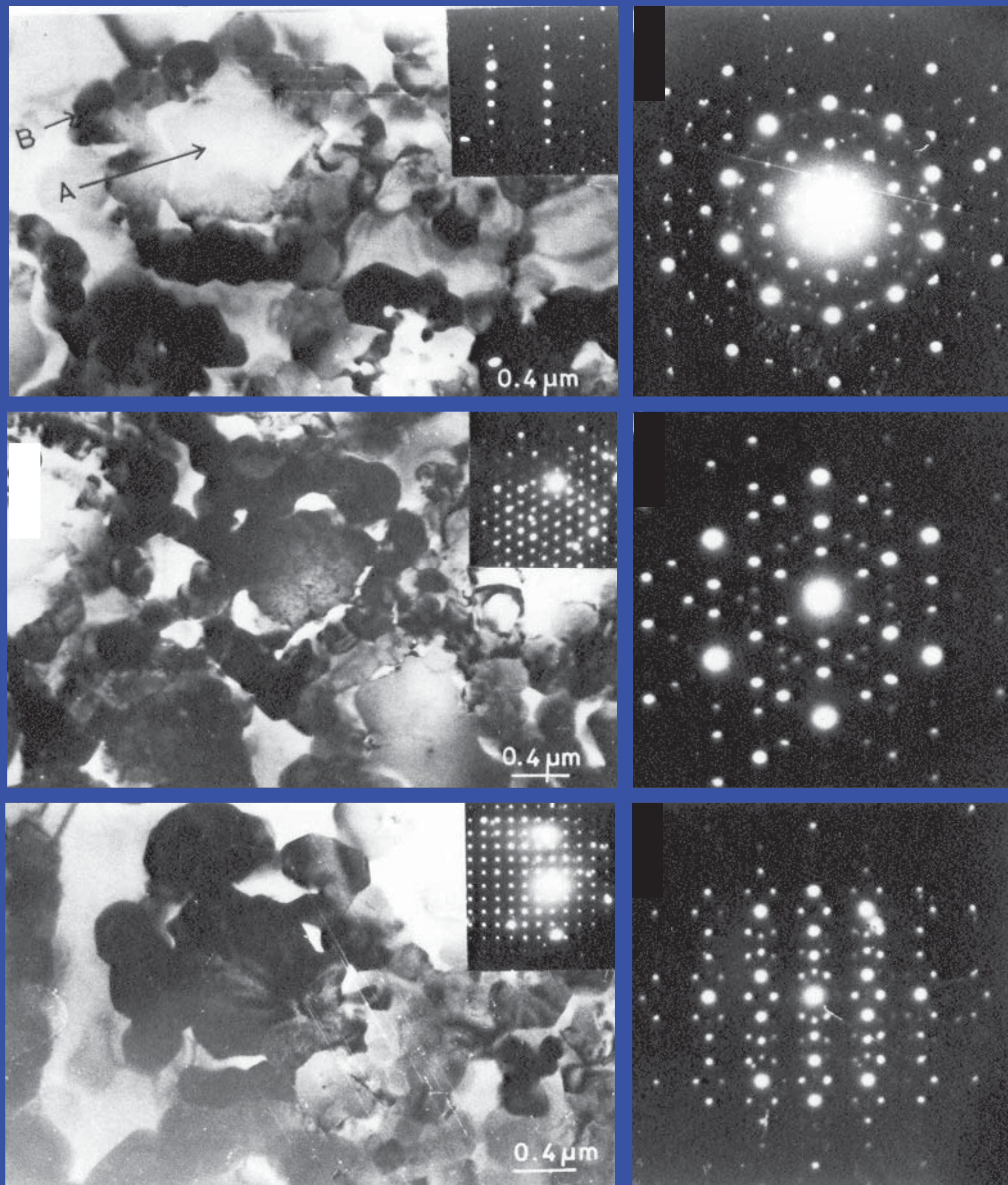

Al-Fe-V-Si alloy showing growth morphology of icosahedral phase surrounded by crystalline ring along 5-, 3- and 2- fold axes

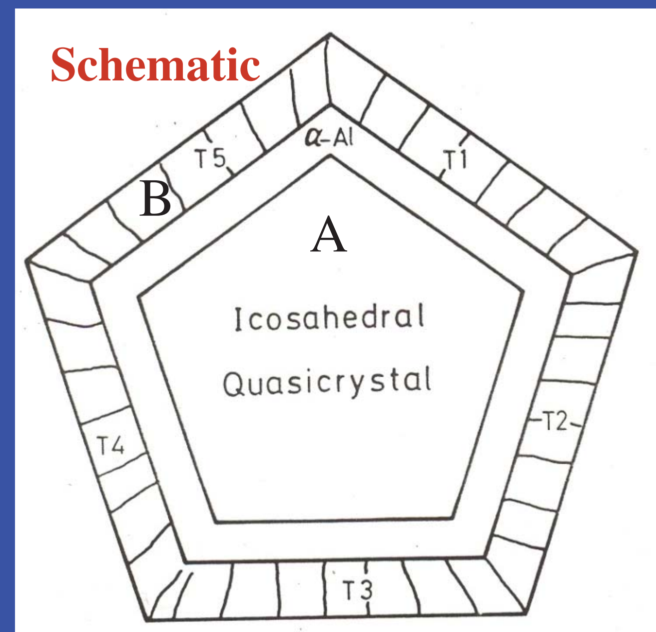

Formation of icosahedral phase surrounded by cubic silicide particles

Acta Materialia 1996

J. Mater. Res. 2001

Quasicrystals:

Nobel Prize in Chemistry – 2011 (5th October)
Professor Daniel Shechtman, Israel Institute of Technology
Date of birth: 24th January 1941, Observation: 5th April 1982

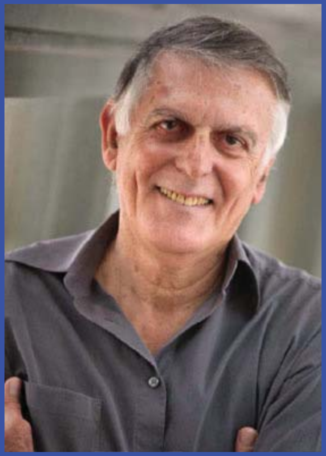

D.Shechtman, I.Blech, D.Gratias, J.W.Cahn, *Metallic Phase with Long-Range Orientational Order and No Translational Symmetry*, Physical Review Letters, 53, 12 November 1984

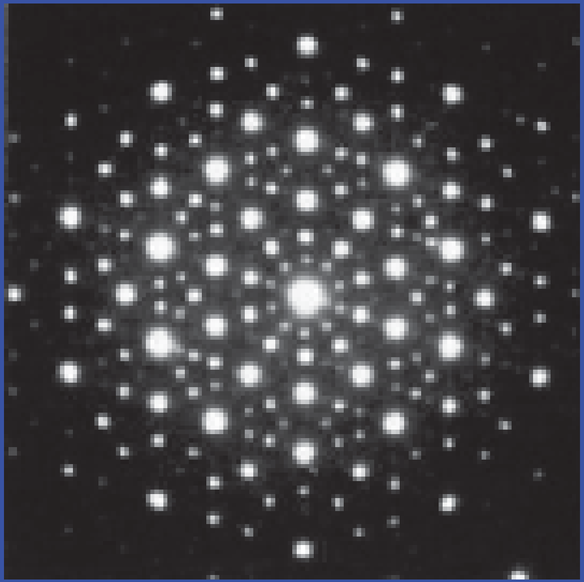

SAEDP along 5-fold rotational symmetry recorded from a single grain of the icosahedral phase

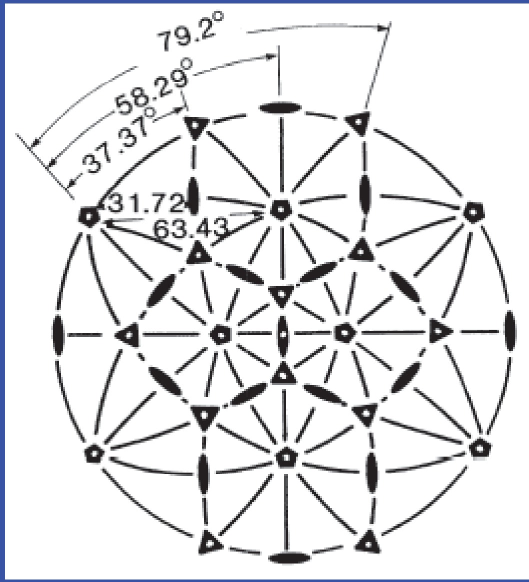

Stereographic projection of the symmetry elements of the icosahedral point group $m\bar{3}\bar{5}$

Nanostructured bulk spray atomized and deposited AZ_{31} magnesium alloy (Mg-2.8Al-0.84Zn-0.2Mn-0.15Si-0.007Cu-0.005Fe-0.004Ni in wt.%)

Mater Sci Tech 2010

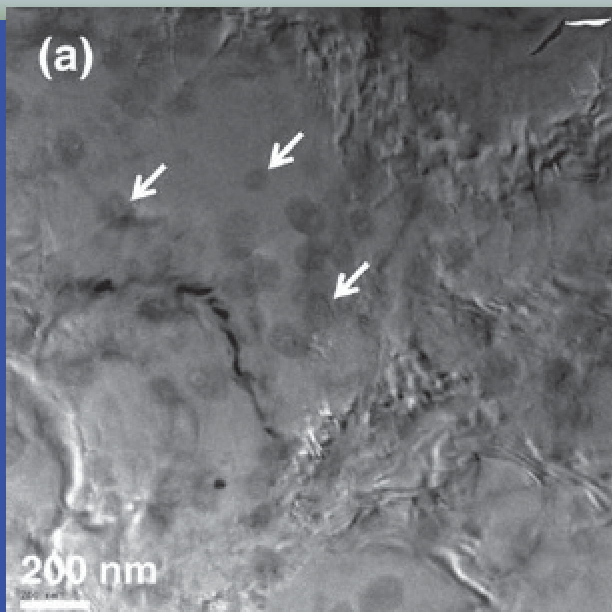

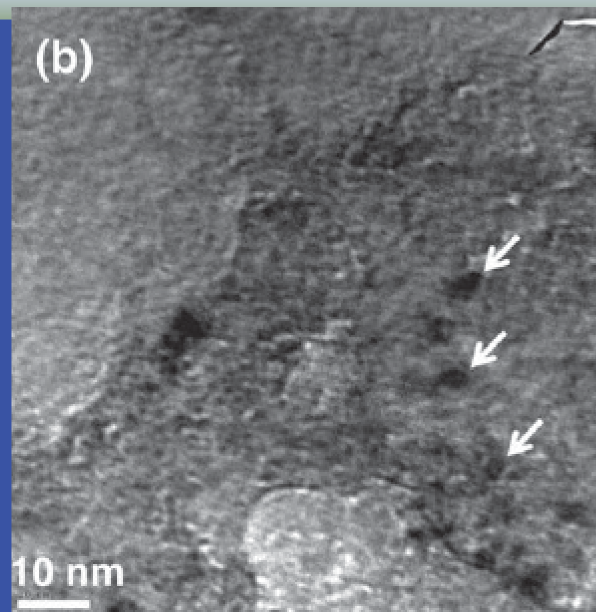

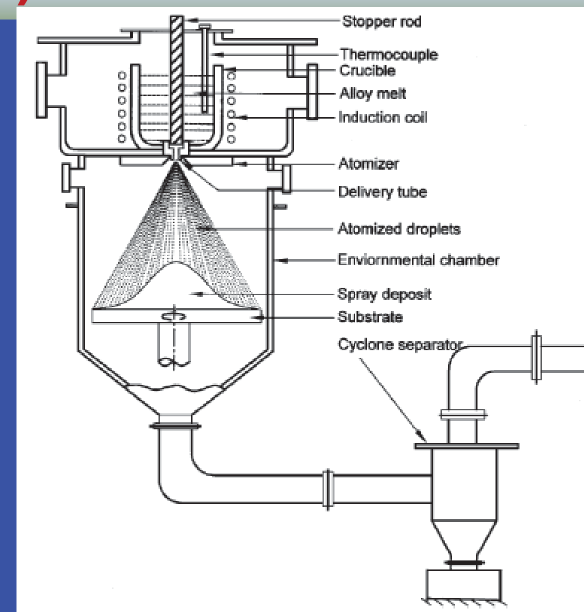

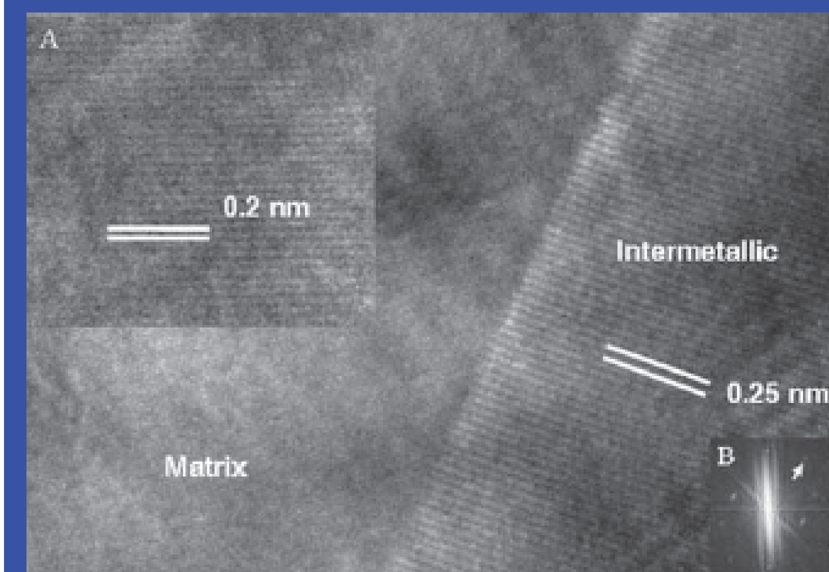

Orientation relationship between $Mg_{17}Al_{12}$ and Mg:

[1120]Mg // [111] $Mg_{17}Al_{12}$

***hkl*: 411, d=0.25 nm, cubic**

***hkl*: 1012, d=0.2 nm, hexagonal**

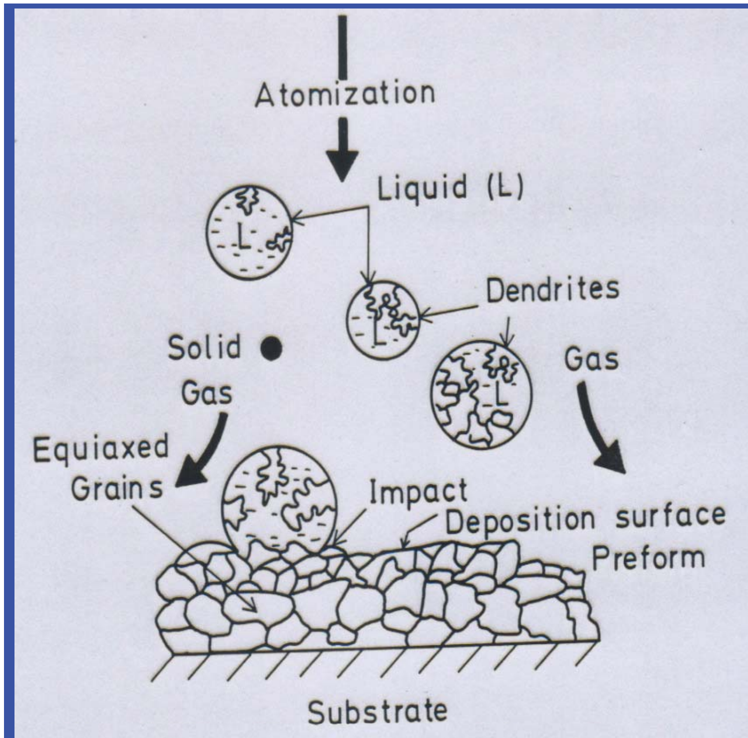

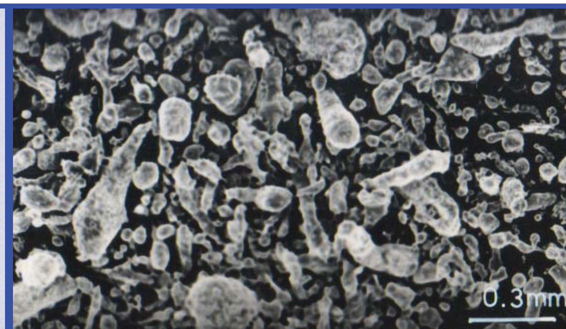

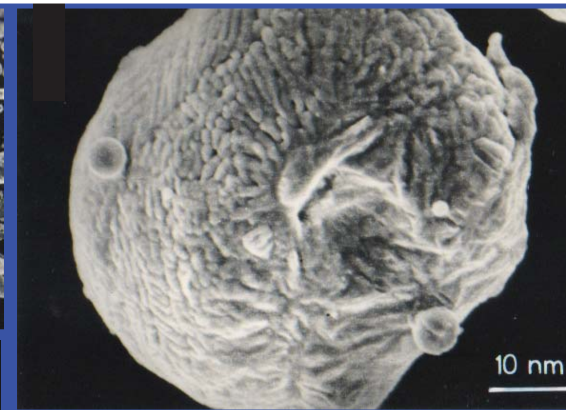

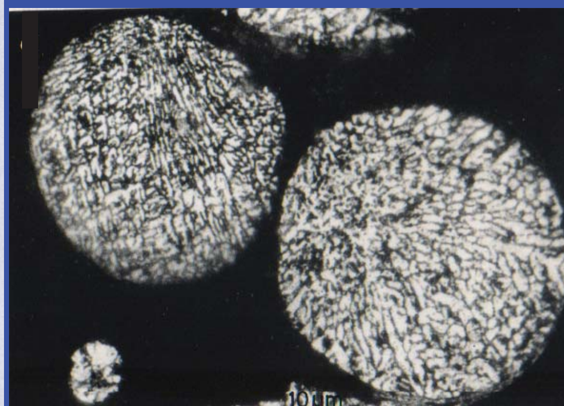

Size of droplets and powder particles

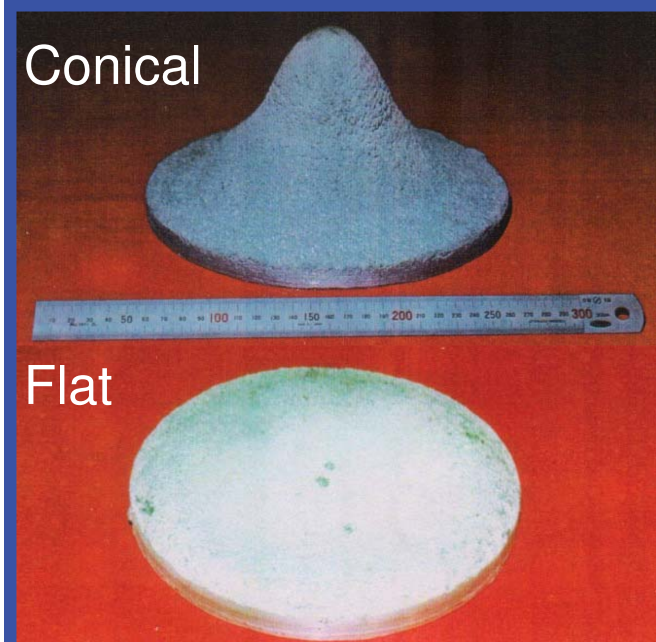

Microstructure of Spray deposits

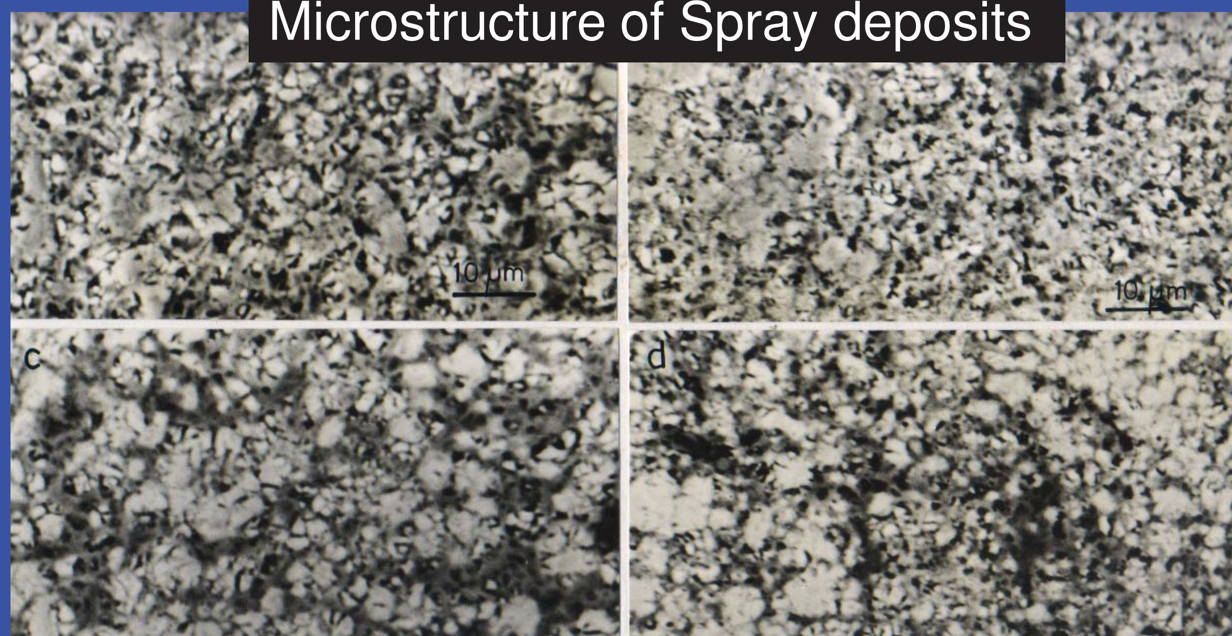

Spray dynamics and heat flow characteristics

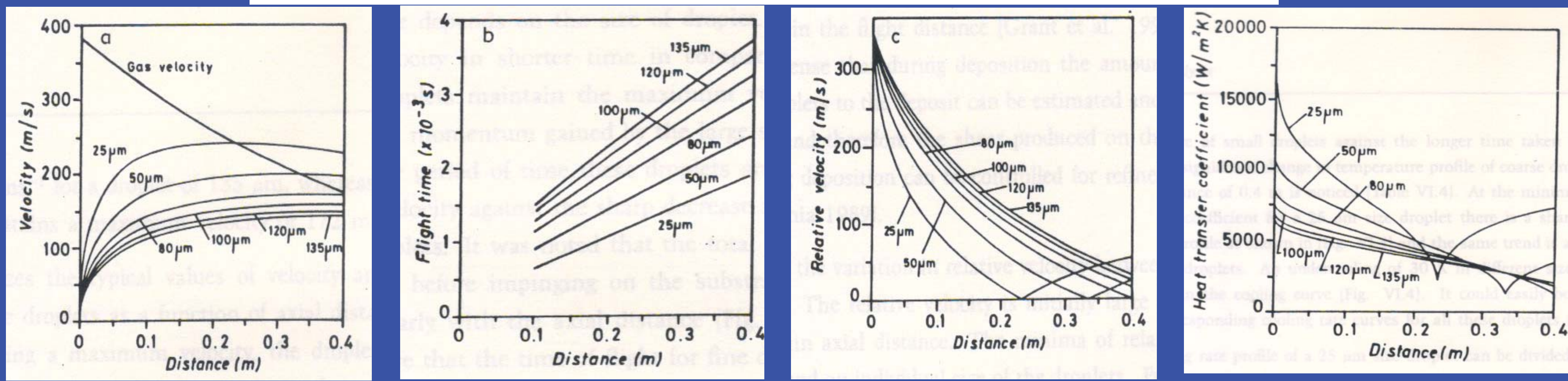

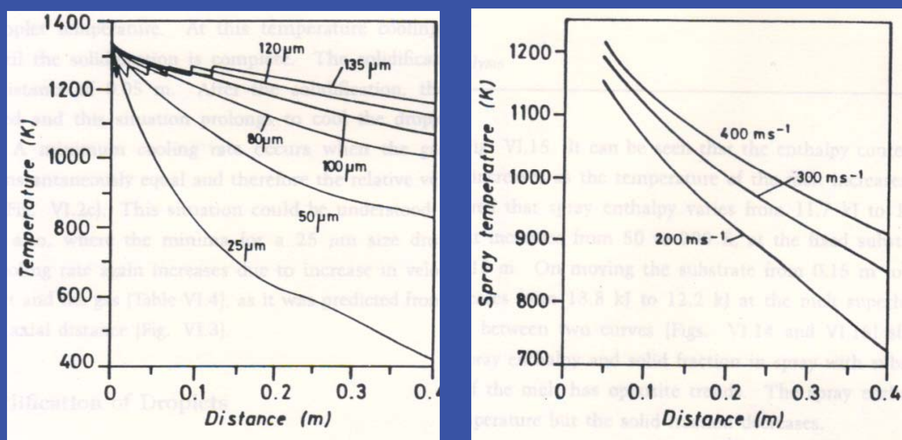

During Gas Atomization

During Spay Deposition

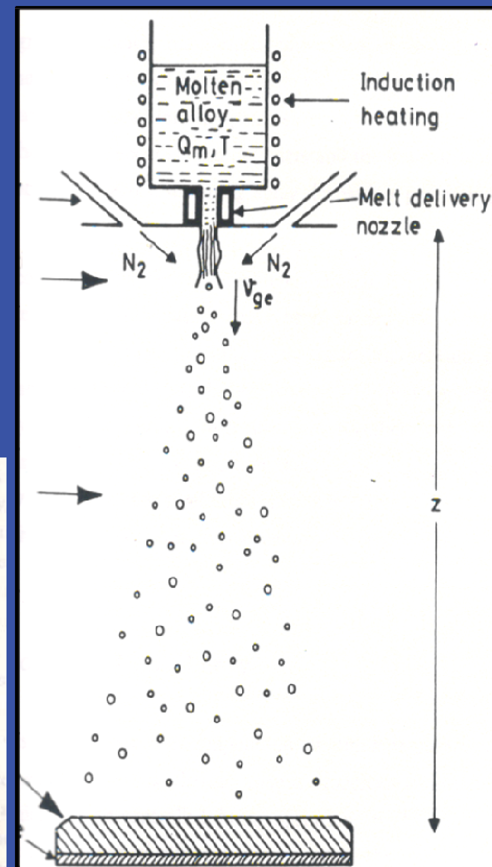

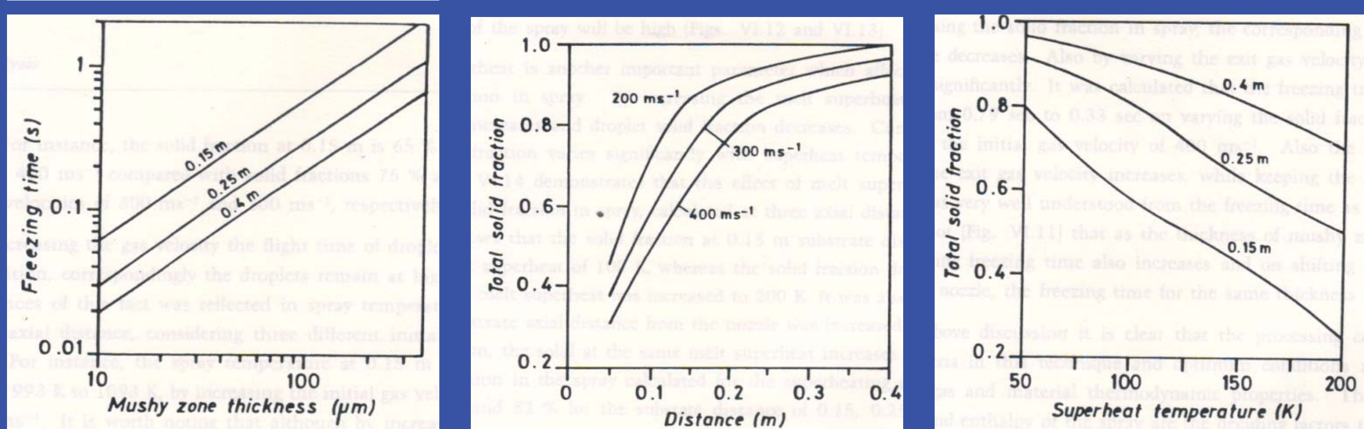

Synthesis and Characterization of Al-alloy/SiC_p nanocomposites employing high energy ball milling and spark plasma sintering

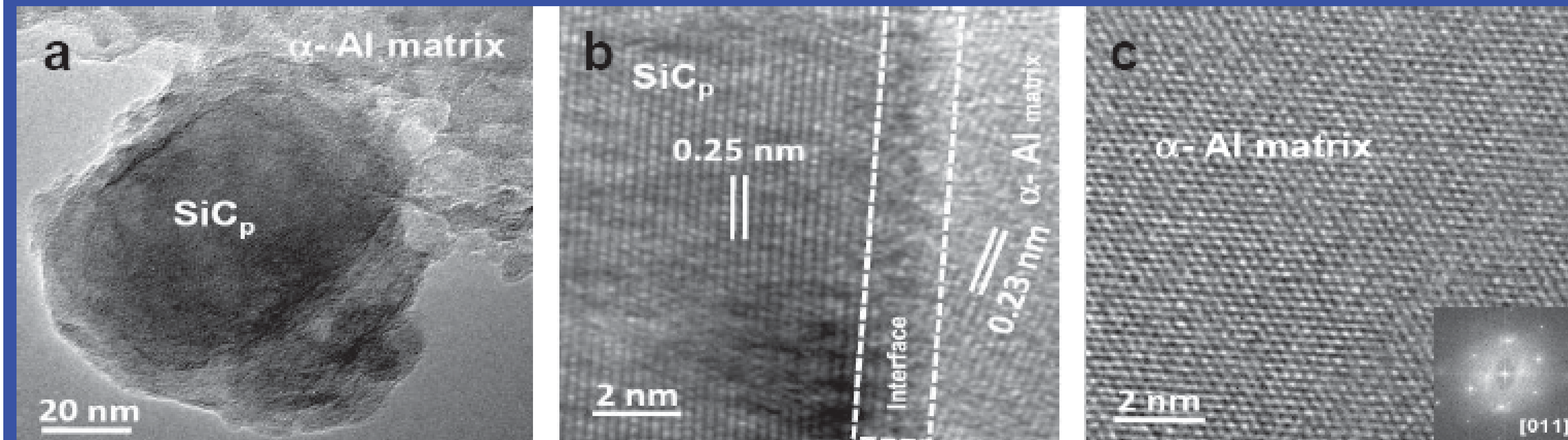

HRTEM images of spark plasma sintered Al-5083/10 wt.SiCp nanocomposite; (a) large number of nanocrystalline grains over entire matrix of Al-alloy and SiCp, (b) interface at atomic scale between Al alloy matrix and SiCp and (c) lattice imaging of Al alloy matrix

XRD patterns

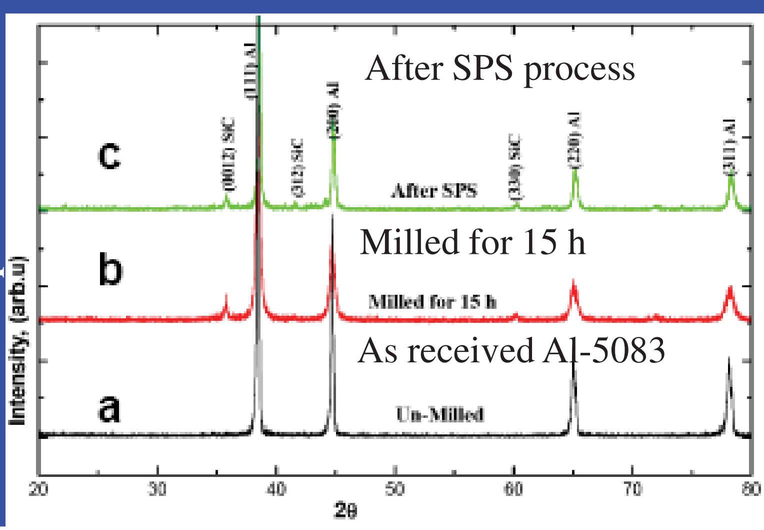

Nano-indentation

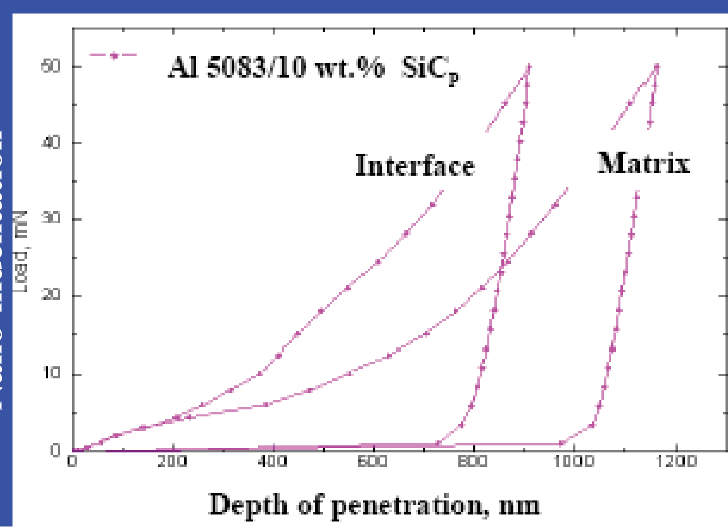

Advanced Materials Research 2012

Cross sectional images at different annealing treatments

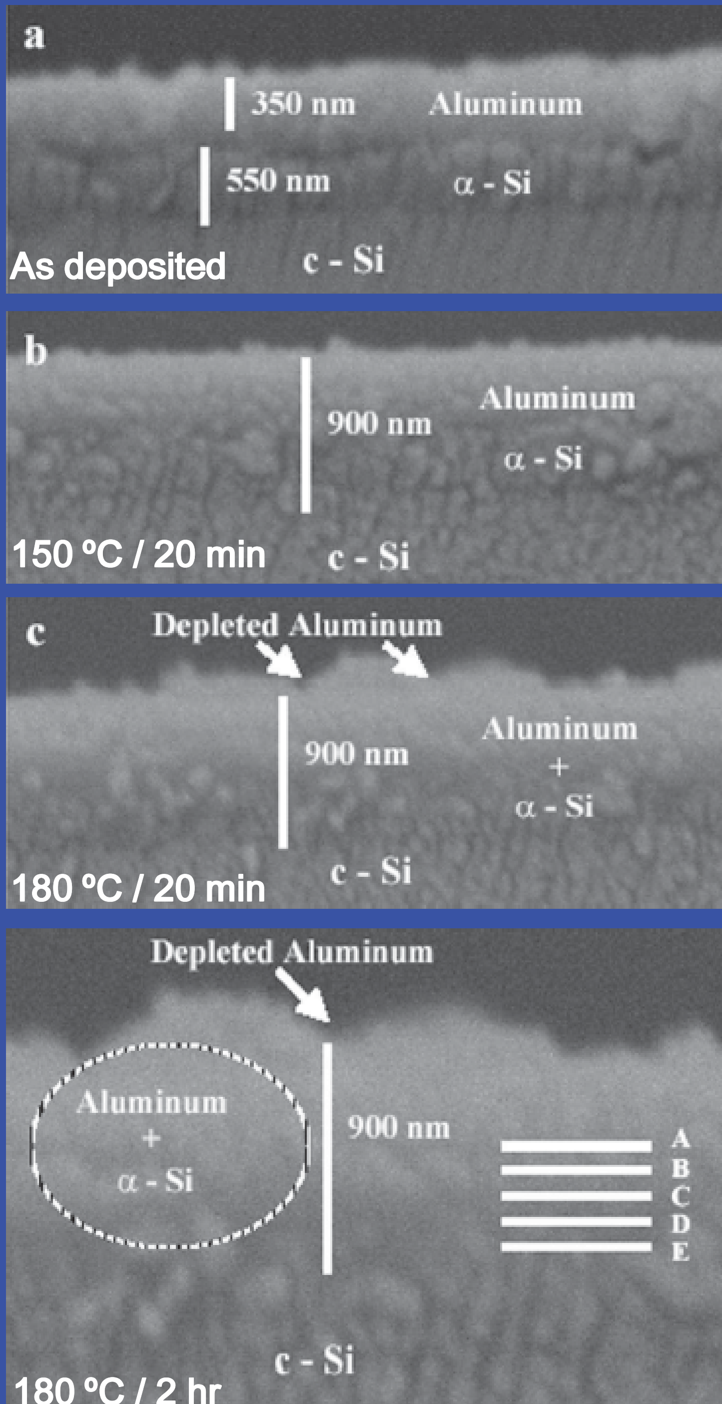

Metal induced crystallization of Amorphos Si

In-situ Annealing experiments

(DST-NSF)

Mechanism for Crystallization

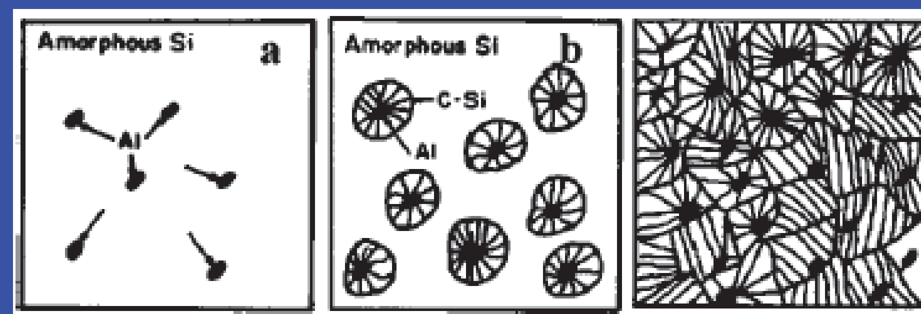

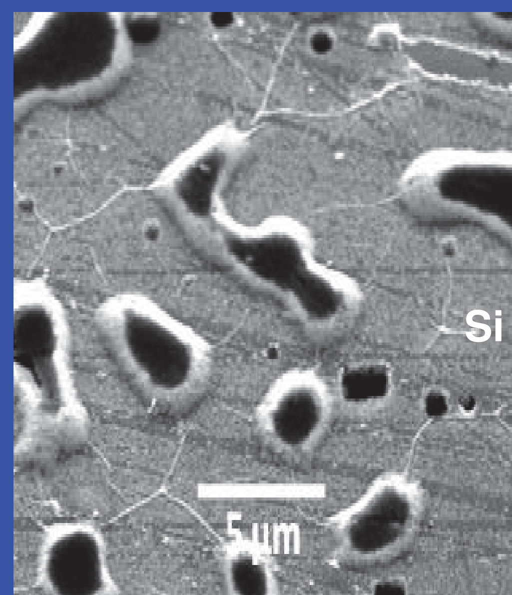

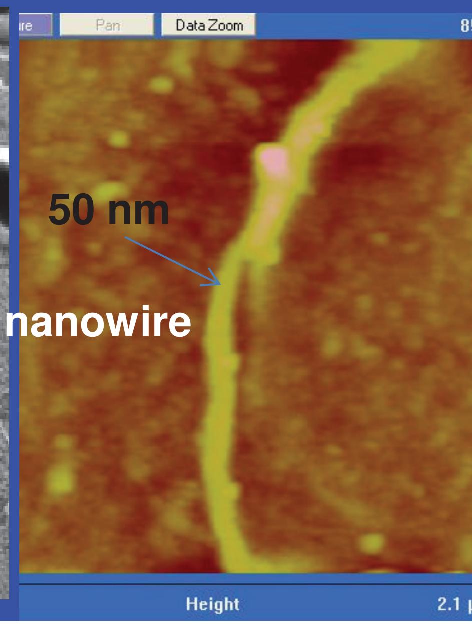

Oxide Nanostructures

Oxide nanomaterials like ZnO, CdO, TiO_2 , WO_3 , In_2O_3, SnO_2 show enormous potential applications in device fabrications. Their properties can be tailored significantly by producing them at micro- and nano-scale in different morphologies.

ZnO (Zinc Oxide)

CdO (Cadmium Oxide)

CuO (Copper Oxide)

TiO_2 (Titanium Oxide)

WO_3 (Tungsten Oxide)

Al_2O_3 (Alumina)

Application	CdO	WO_3	ZrO_2
Electronic devices	Used in photodiodes, phototransistors, photovoltaic cells, transparent electrodes,LCDs, IR detectors, cadmium plating baths, electrodes for storage batteries, phosphors etc.	Used in electrochromic windows or smart windows, flat panel displays, optical memory, writing reading erasing devices, electronic information displays, optical modulation displays, x-ray screen phosphors, fireproofing fabrics etc.	as a solid electrolyte, di-electrolyte, in transparent TFTs, nano-lithography, Precision valve balls & seats, Fuel cell membranes, High temperature induction furnace susceptors, Marine pump seals & shaft guides, Electric furnace heaters over 2000°C
Ceramics & coatings	Used in pigments and as ceramic glages, used in anti-reflection coatings.	Used in pigment in ceramics	In thermal barrier coatings, protective coatings for electronic devices, Powder compacting dies,
Sensing	Has potential applications in LPG sensors, formaldehyde sensors, ethanol sensor. Its composite has utility as CO sensor.	One of the best sensors for reducing gases such as NO_2,CO and H_2,also used in humidity and temperature sensors	Used in oxygen sensors, pollutant gases like Ammonia and CO can also be detected.
Catalysis	catalyst in ethanol dehydration, in chemo-regioselective reactions	Used as a photocatalyst in water splitting	In photocatalysis, as a general catalyst in knoevenagel condensation reactions
Bio-applications	Used as a nematocide	It has potential application in the detection of lipids and peptides	Its composites can be used in various biological load bearing applications

Application	ZnO	TiO_2	CuO
Electronic devices	used in varistors, phosphors for CRT displays, electroluminescent panel displays,phosphors inside fluorescent tubes, field effect transistors, piezoelectric nanogenerators, in dye-sensitized solar cells	Used in capacitors, reflectors for incandescent lamps, semiconductors, bragg-stack style dielectric mirror, dye sensitized solar cells,memresistors, electronic data storage medium	Used as a major component in superconductive materials, as an anode material in Li ion batteries, magnetic storage devices, field emission sources,solar cell devices, optical switches
Ceramics & coatings	Used in UV protecting clear coats, antifungicide for paints, powder coating	Used in general pigments and coatings, UV protecting clear coats, automotive pigments, reinforcements for metal-matrix composites, porous membrane for gas filtration	Used as a pigment in ceramics to produce blue, green and red colours
sensing	ZnO nanorod based sensors can be used in ammonia, CO, hydrogen and UV detectors, ethanol sensors, Oxygen sensors,	In Oxygen sensors, hydrogen sensors	Used in hydrogen peroxide and glucose sensing, in H_2S sensors , NO_2 sensors and in CO gas sensors
Catalysis	Used as a general catalyst in various reactions, as a visible light photocatalyst,	Used as a general catalyst in various reactions, as a photocatalyst and also as a catalyst support	Used as a catalyst in methanol synthesis , alkene oxidation, used as a photocatalyst
Bioapplication	Has potential applications as an antibacterial agent, bio-imaging on plant cells,intracellular potentiometric ion sensors, owing to its sensitivity towards tiny forces ZnO based pressure sensors can be produced and implanted in the body due to its biocompatibility, can be used as a glucose sensor, used in plasmid DNA delivery,	Its presence increases implant bioactivity and osteoblast adhesion of Ti and its alloys, enhances blood coagulation by reducing clotting time , acts as a biosensor for amperometric detection of glucose, enhances apatite formation, drug elution, cell activity and the nanotube arrays play important role in protein separation and drug delivery, TiO_2 sol-gel has been used to detect large proteins like trypsinogen and also in the detection of insulin, can be used in the destruction of airborne pathogen	CuO based nanostructured surfaces can be functionalized to produce superhydrophobic interfaces for digital microfluidic systems for physical transfection of cells, has potential application as a biocidal agent,
others	Used in cosmetics like footcare, OTC optical and ointment,	Used in cosmetics such as sunscreens, moisturizers, lipstick,	Can be used as a crucial material for ink-jet printing

Novel Growth Morphologies CdO

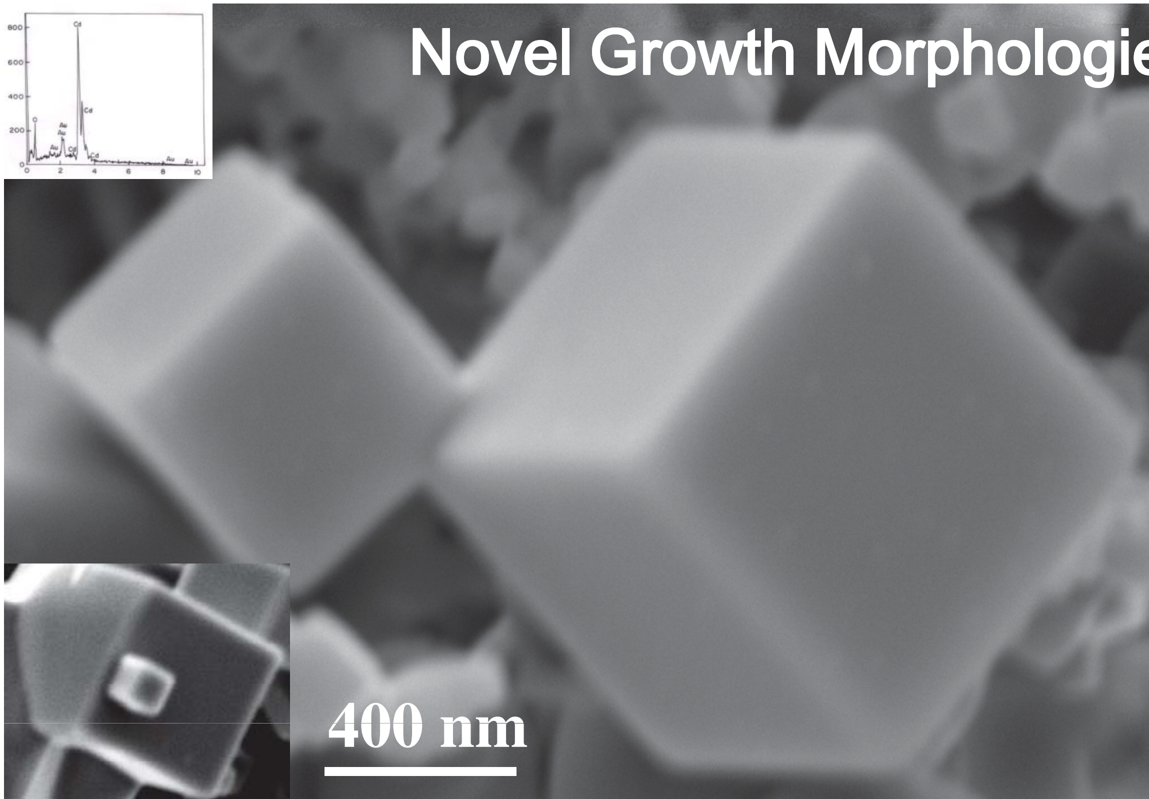

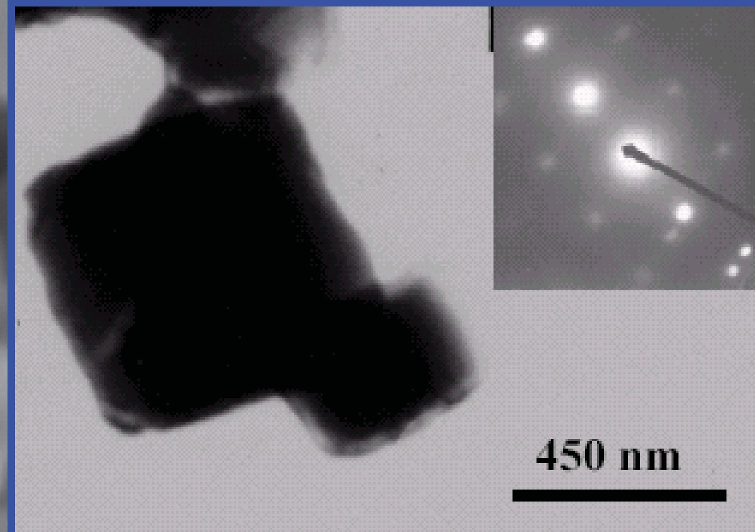

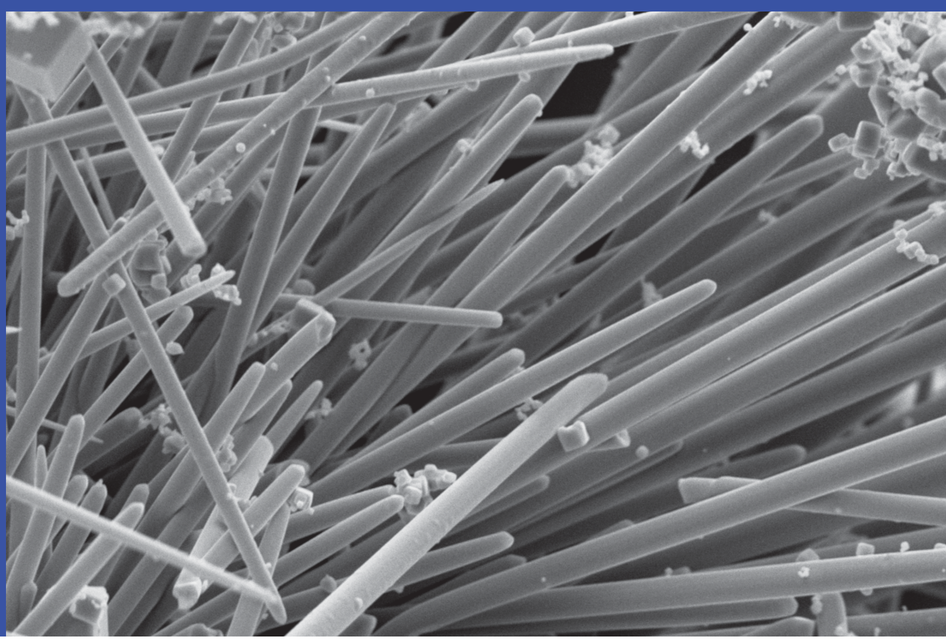

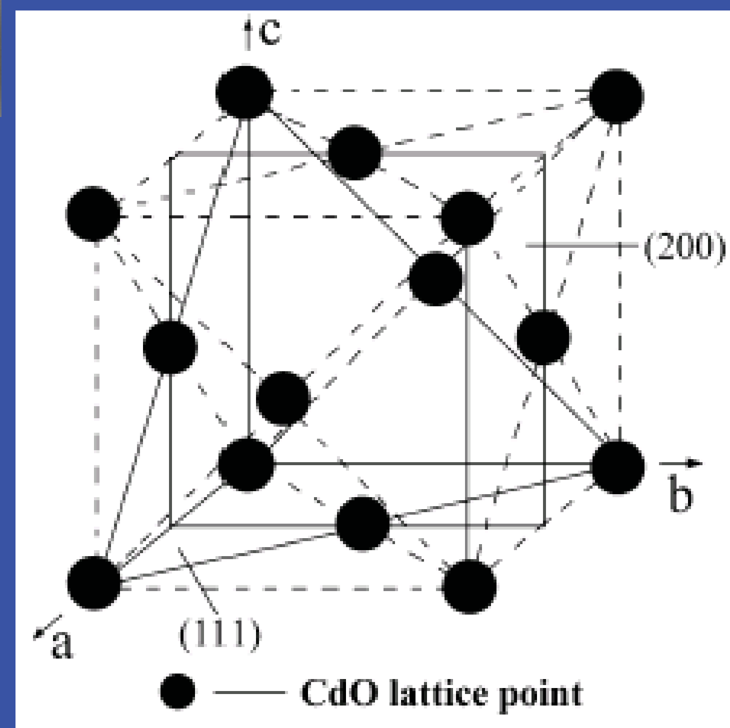

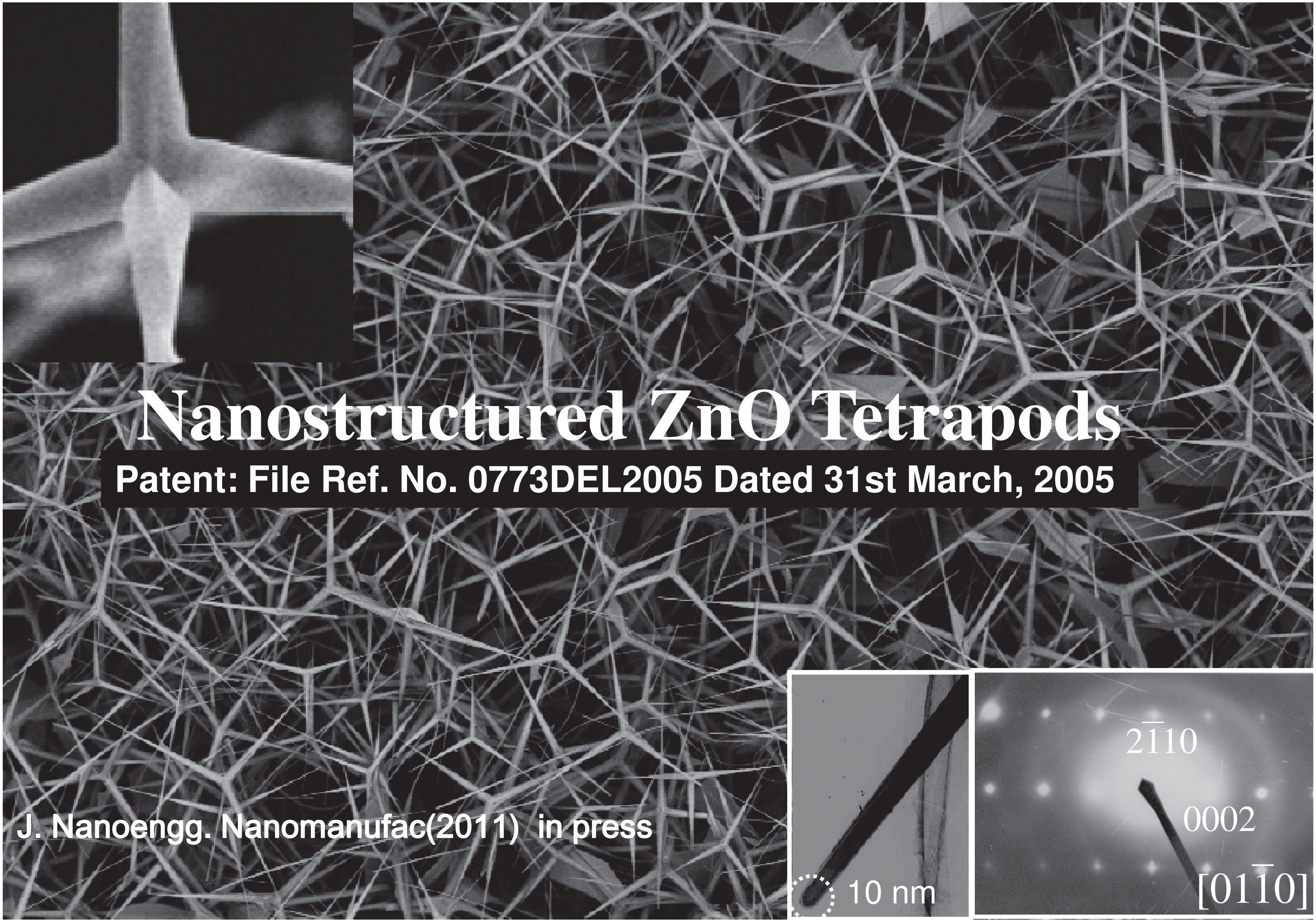
Nanostructured ZnO Tetrapods
Patent: File Ref. No. 0773DEL2005 Dated 31st March, 2005
J. Nanoengg. Nanomanufac(2011) in press
10 nm
$2\bar{1}10$
0002
$[01\bar{1}0]$

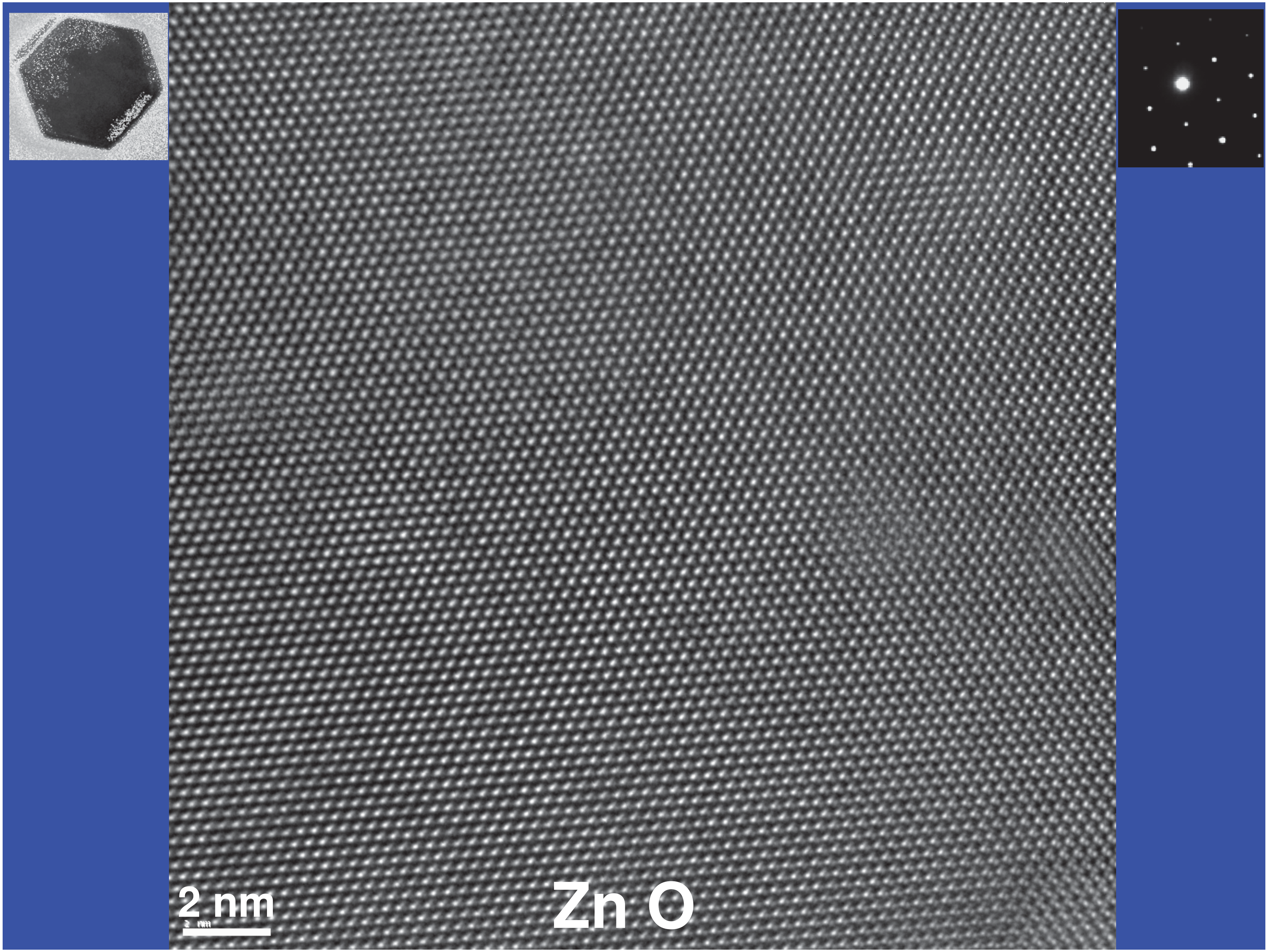
2 nm
Zn O

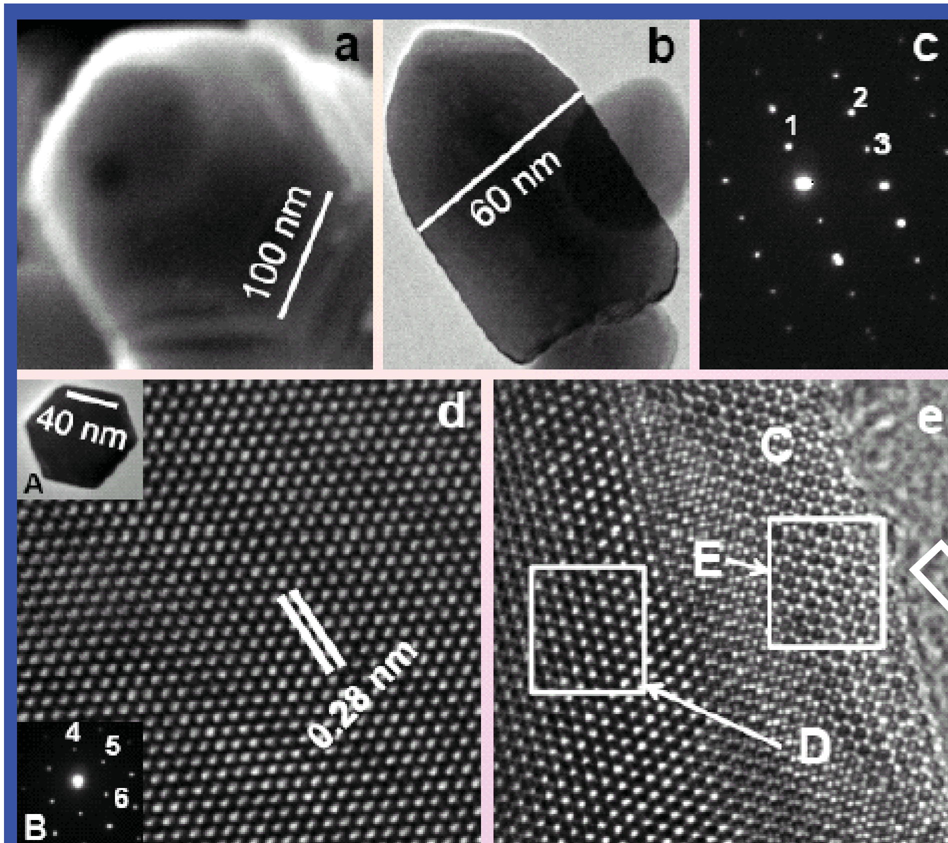

Structural determination of Zn-O dumbbells in facetted nano-particles

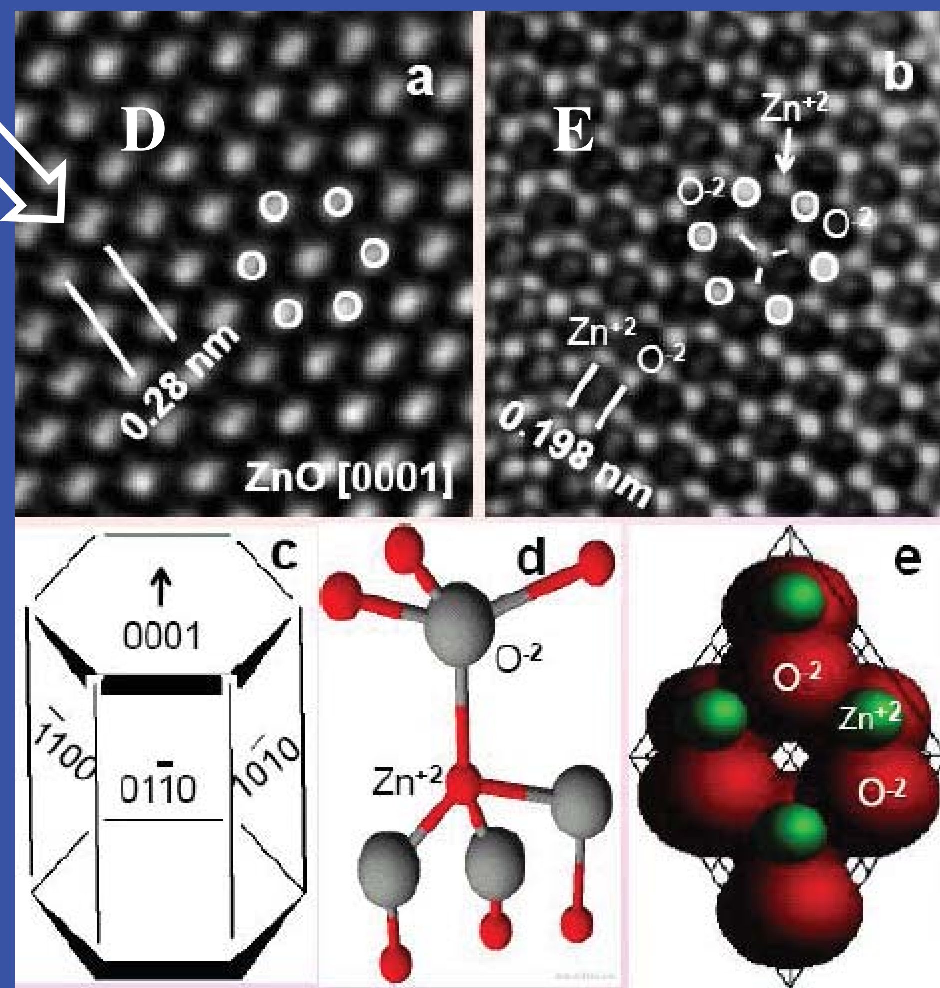

First practical examination of Zn-O bond length of approximately 0.198 nm in real space

Book Chapter: A. Mendez Vilas, Ed. Microscopy: Science, Technology, Applications and Education, Formatex Research Center, Spain (2010) vol. 3 No. 4, 1820-1823

Tunable emission bands in nanostructured $Zn_{1-x}Fe_xO$

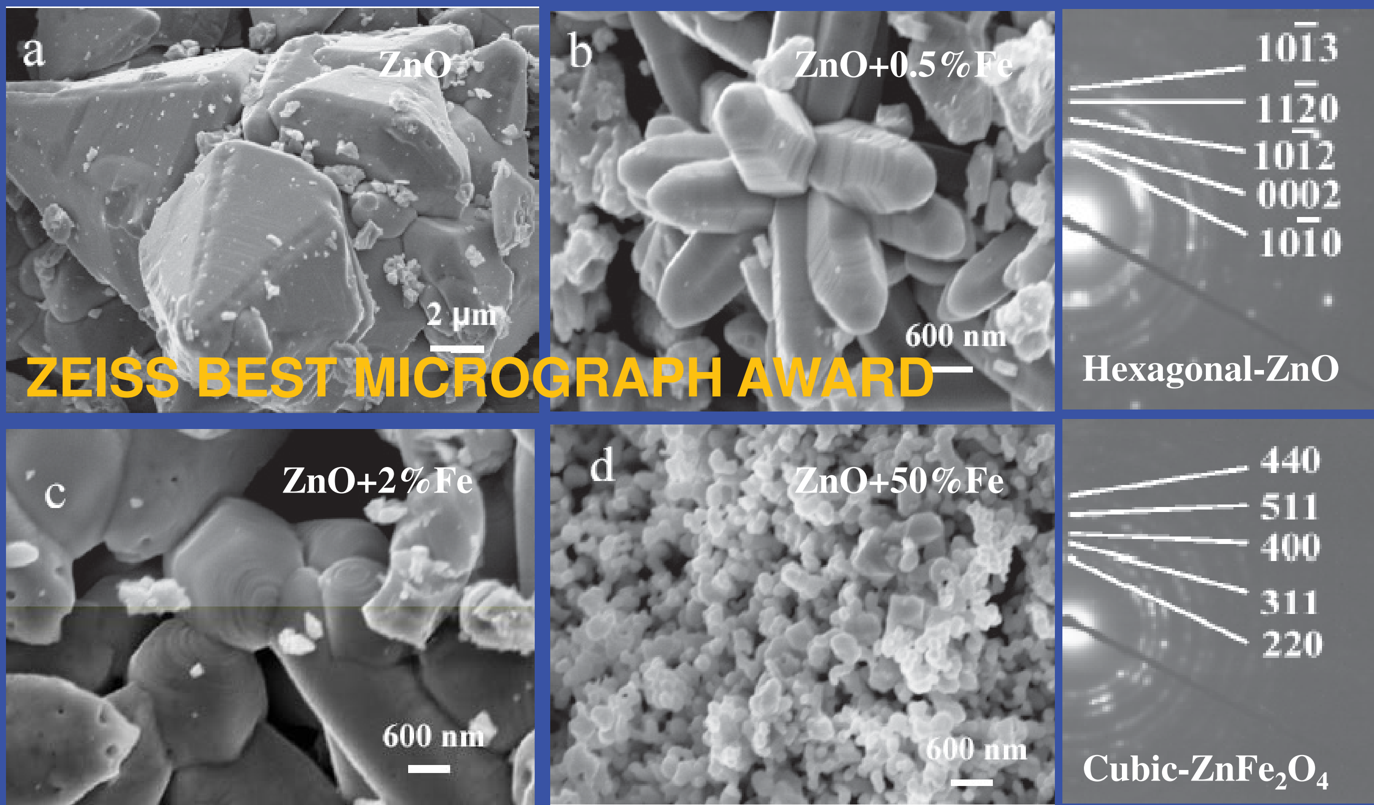

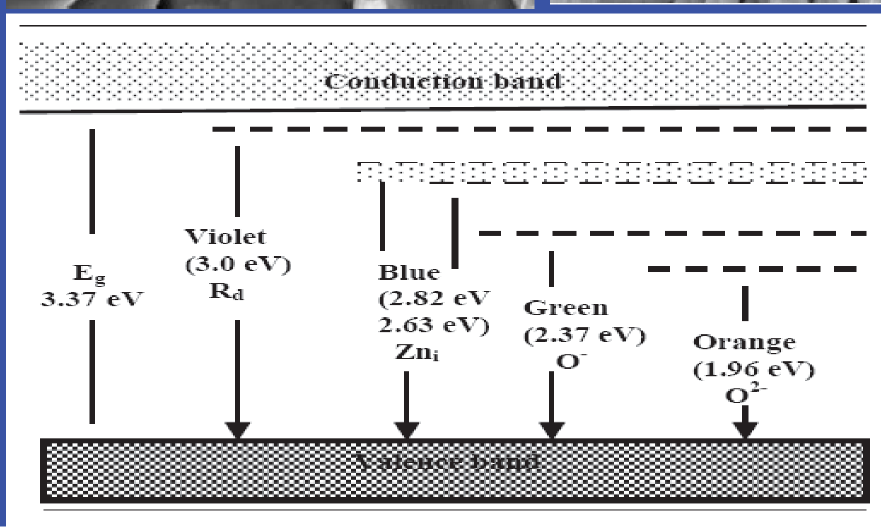

Orange (632nm)

Green (523nm)

Blue (468, 440nm)

Violet (412nm)

ZnO → (Zn,Fe)O

JNN (2007), NRL (2007), IEEE Sensor (2008), Nanotech.-book (2008), MCP (2009)

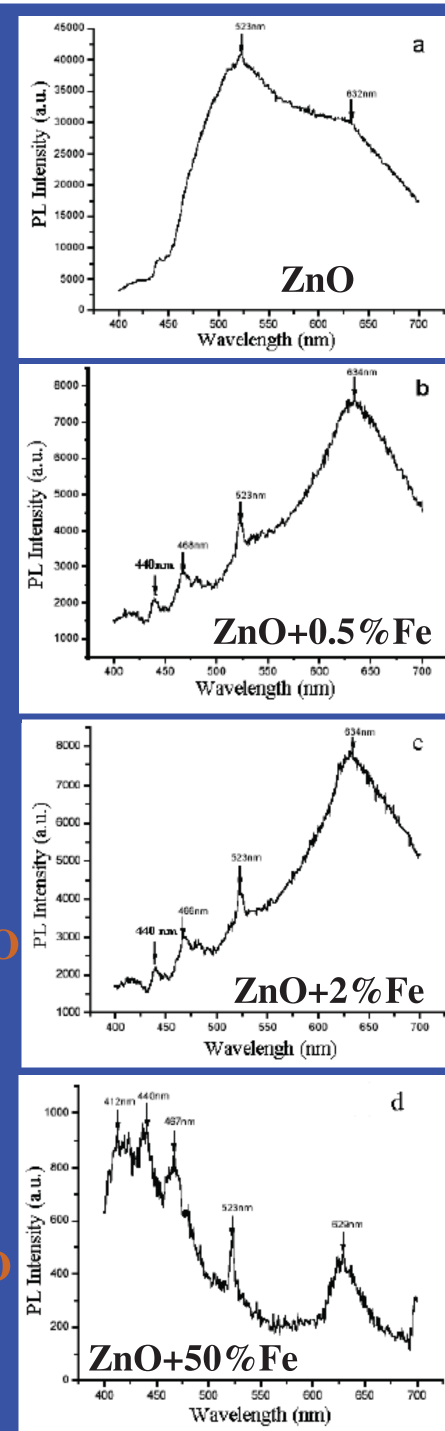

Thermoluminescence

The thermally stimulated luminescence technique, commonly termed as thermoluminescence (TL). The ZnO is good for thermoluninescence dosimeters (TLD) applicable as environmental dosimetry, clinical dosimetry, inside nuclear reactors, during food sterilization and materials testing.

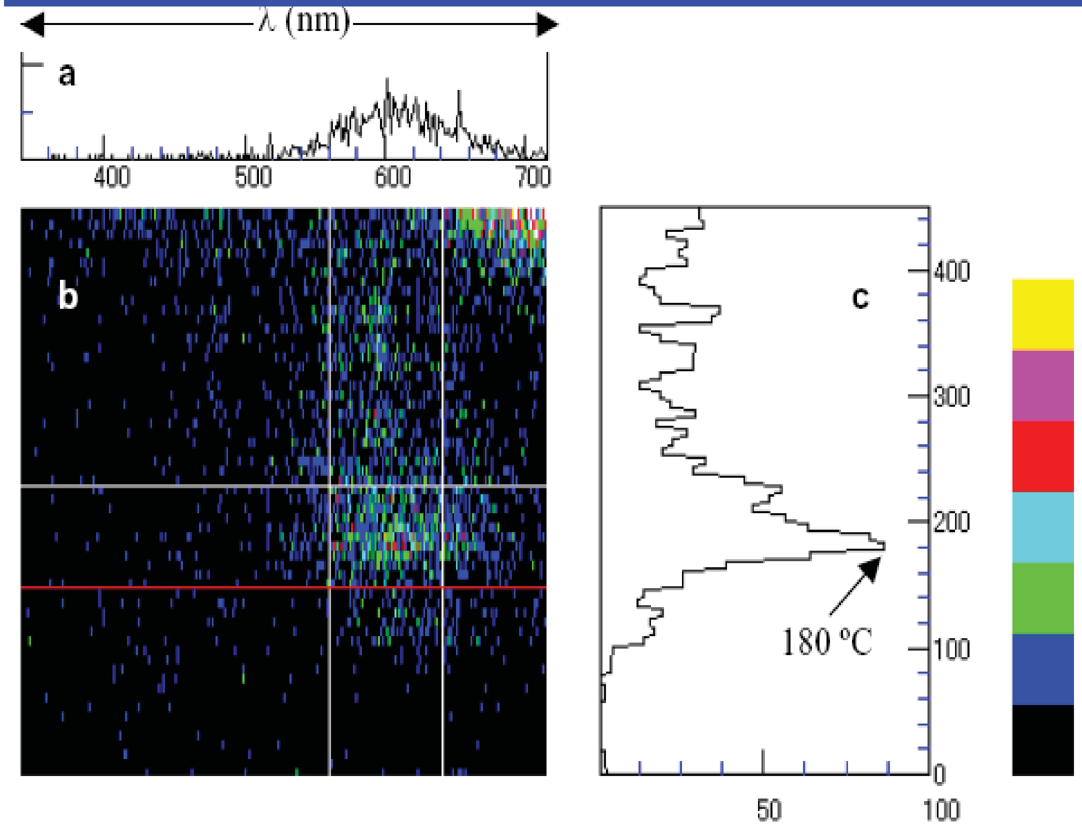

Induced TL spectra of an undoped ZnO sample at various temperatures. It shows a TL peak around 180˚C around 600 nm. (a) TL spectrum integrated between 150 and 230 ˚C (b) spectrum-temperature diagram. TL intensity is displayed b false colors. © TL glow curve integrated between 560 and 640 nm, *Optical Mater 2009*

WO_3: crystal structure , microstructure and performance

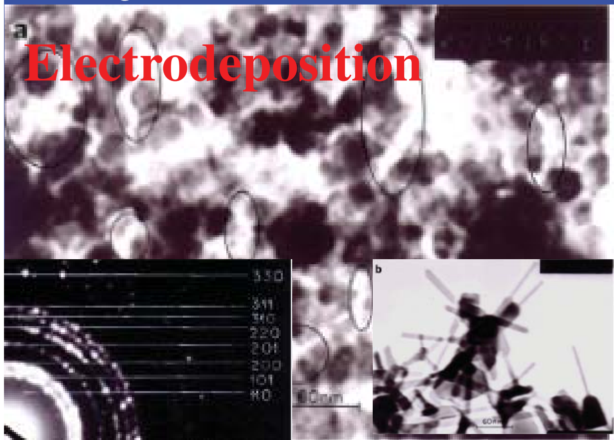

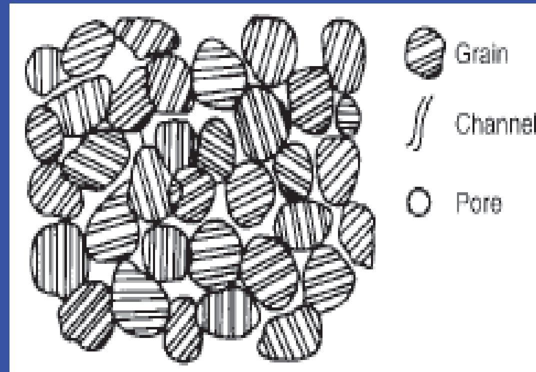

Nanotechnology (2006)

a=0.53, c=0.37 nm

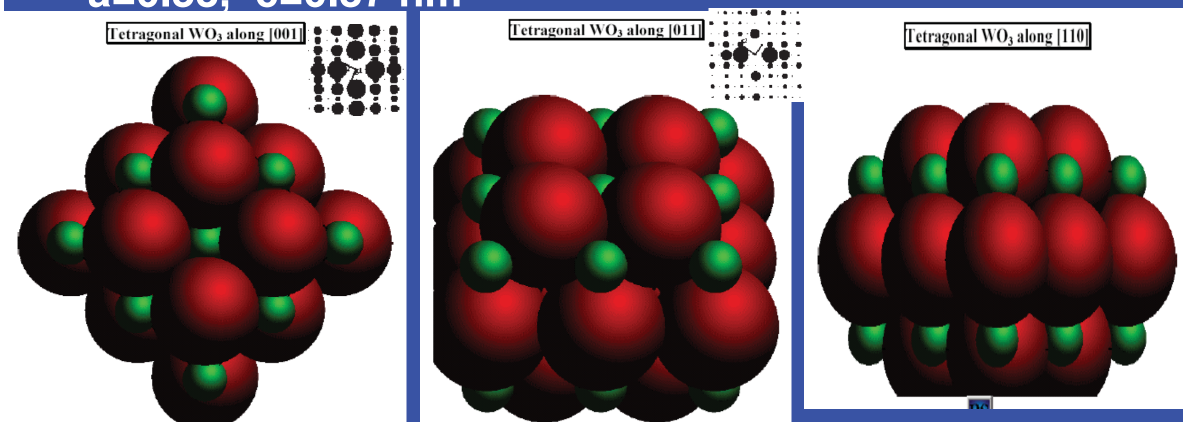

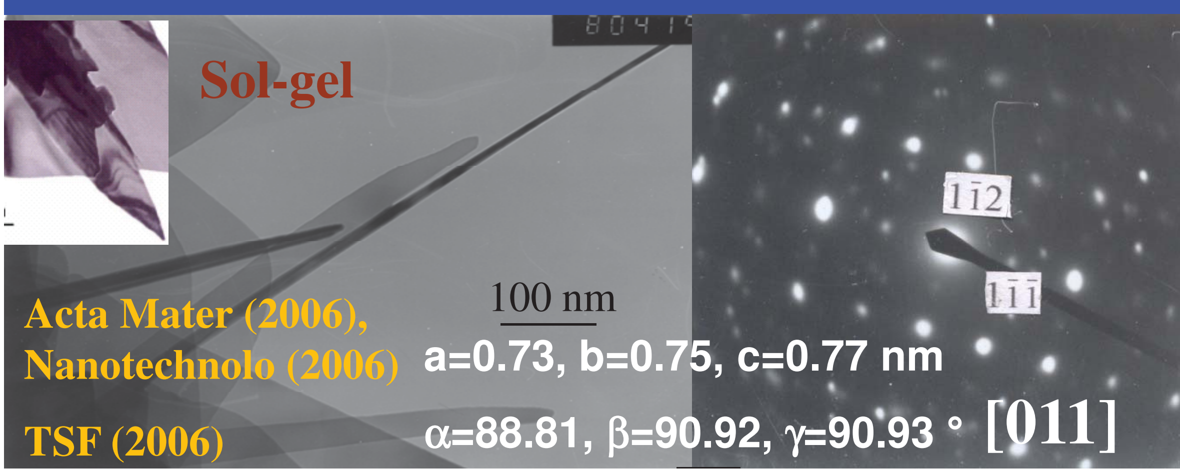

Acta Mater (2006),
Nanotechnolo (2006)
TSF (2006)

a=0.73, b=0.75, c=0.77 nm

α=88.81, β=90.92, γ=90.93 °

WO_3 films annealed at 100^0C shows the best electrochromic performance, due to the pentagonal voids of the tetragonal structure, mesoporosity and presence of channel like pores in the film.

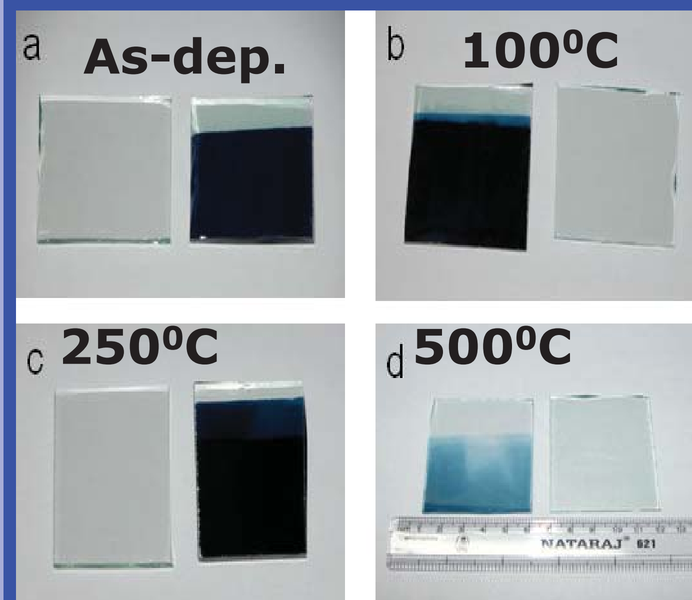

Smarter liquid-crystal display

(J.Phys. D Appl. Phys. 44 (2011) 315404, NATURE India 23 August 2011)

Alumina nanoparticles to trap ionic impurities in ferroelectric liquid crystal (FLC) – based displays, which may improve display resolutions.

FLCs have good optical contrast, low turn-on voltage, memory effect and fast response. Impure ions can be efficiently trapped by Alumina nanoparticles for long durations. FLC materials free from ionic impurities have higher resolution and better contrast

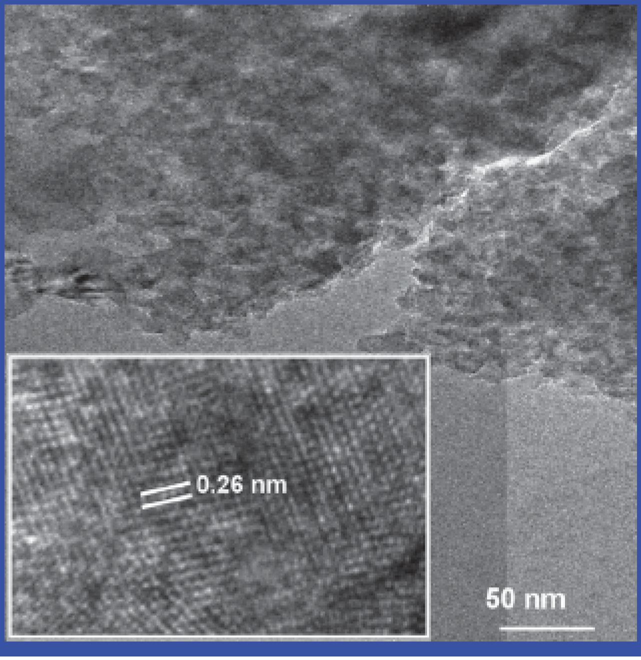

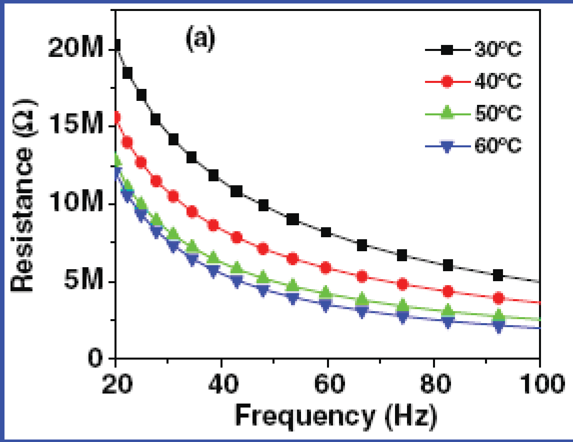

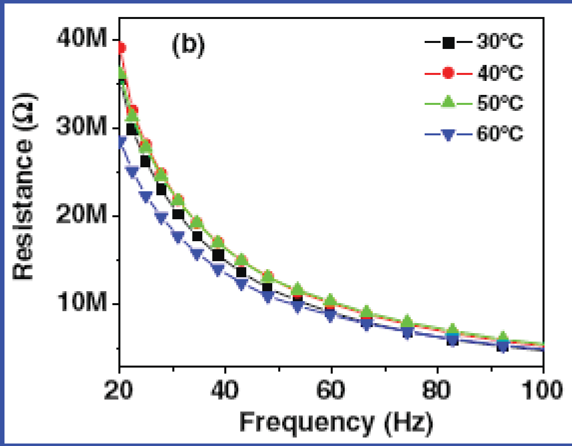

Electrical resistance (R) of (a) pure and (b) 1 wt.% AL-NPs of size 20-30 nm doped KCFLC 7S material with frequency for aligned 4.2 μm thick cells

Complex growth morphologies and characteristic optical bands of nanostructured CuO

CuO has a square planar coordination of Cu atom to neighboring O atoms and monoclinic crystal structure. With a narrow band gap (1.2 – 1.5 eV). uses as: p-type semiconductor, catalyst, gas sensing, crucial component in high temperature superconductors, pigment, electrode material in Li-ion battery and as nano-fluid

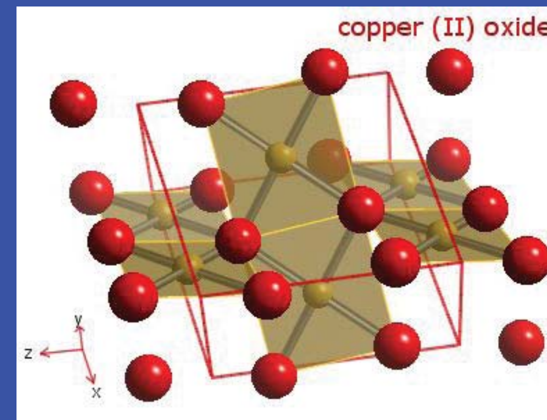

RSC Advances 2011

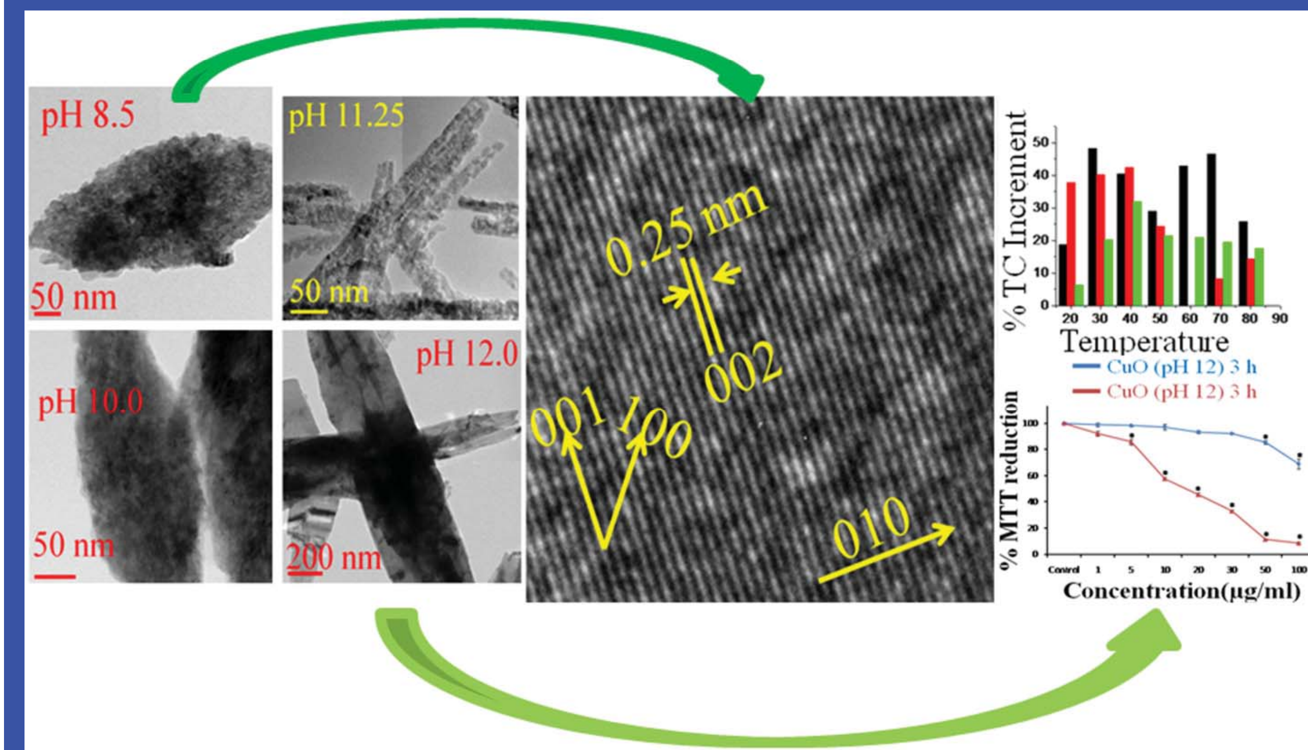

Thermal, luminescence and toxicity were correlated with the shapes of the particles for possible usage in nanofluid and optical devices in conjunction with their biological response.

Toxicity Evaluation of the CuO nanoparticles

Flow cytometric (red fluorescence) quantification of dead *E. Coli* cells after CuO NP treatment; Q2 represents percent dead cells and Q4 represents percent live cells

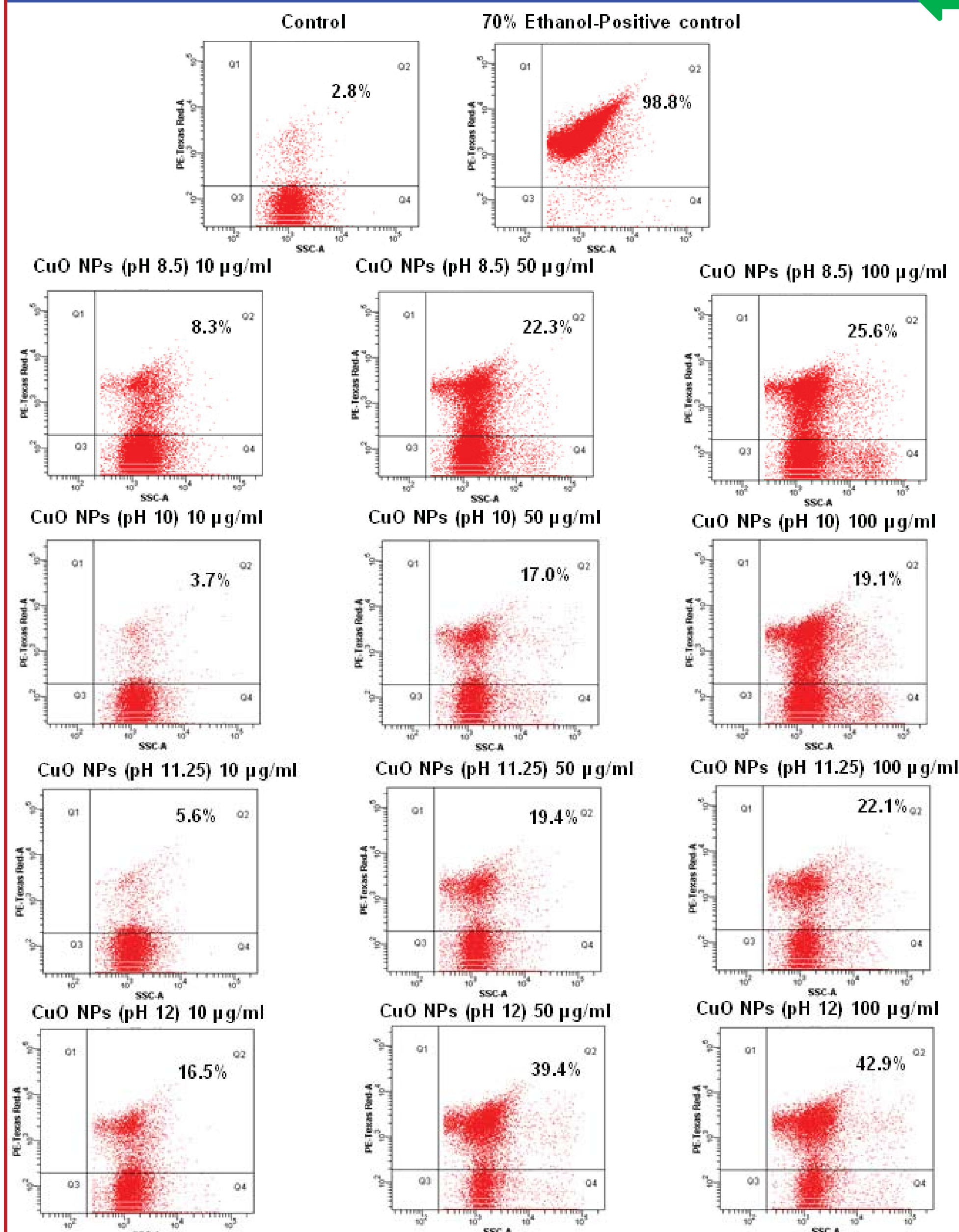

MTT assay is well known method to assess the toxicity of the compound on cellular system under *in vitro* condition. In this assay, yellow tetrazolium MTT dye is reduced by succinate dehydrogenase enzymes produced by mitochondria of the metabolically active cells and form formazan crystal. The spectrophotometric quantification of the solubilized formazan corresponds to the viability of the cells. Our data demonstrates a statistically significant ($p<0.05$) cytotoxic effect of CuO NPs in CHO cells at concentrations 50 and 100 µg/ml after 3 hour exposure. MTT results demonstrated that mitochondrial succinate dehyrogenase activity was reduced to 79% and 38% (relative to 100% of control; pH 8.4) 94%, 45% (pH 10), 79%, 57% (pH 11.25) and 85%, 69% (pH 12) respectively at only the two higher concentrations (50 and 100 µg/ml) after 3 hour exposure

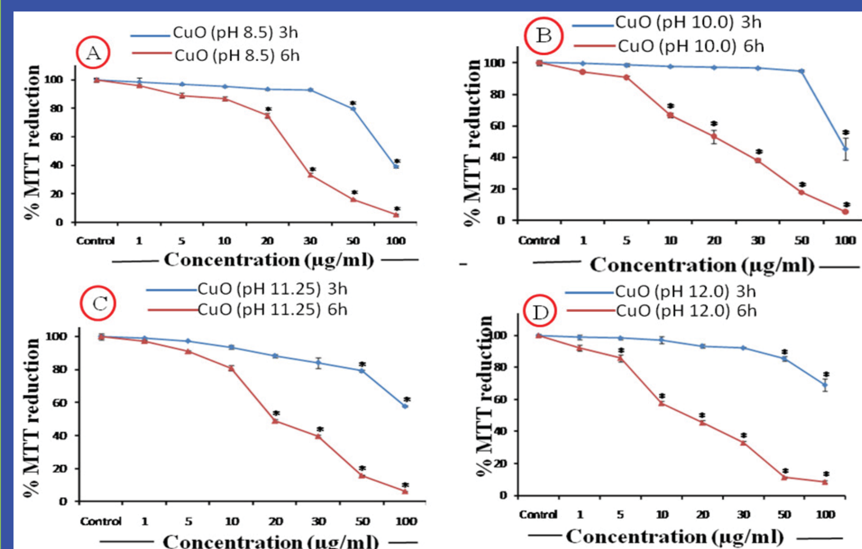

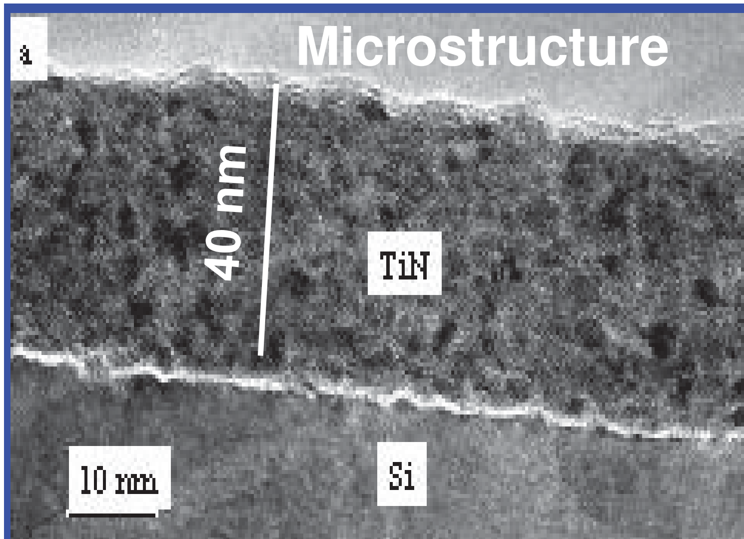

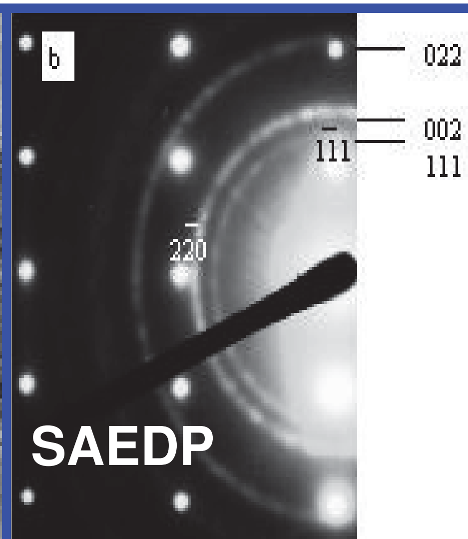

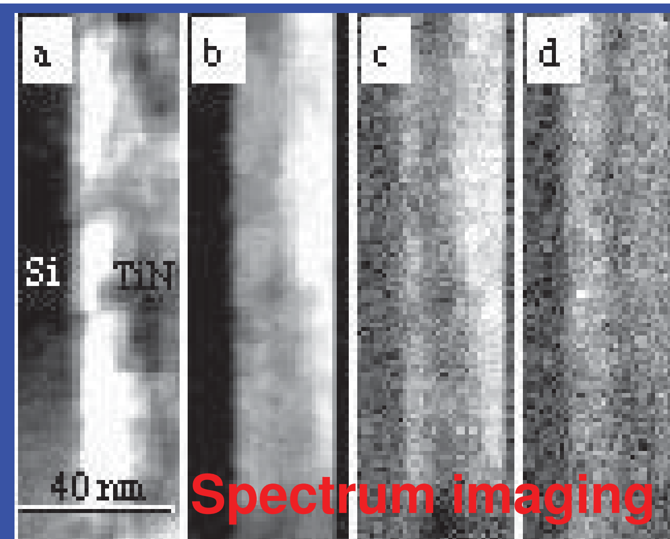

Cross sectional TEM images & analytical measurements: TiN film grown on a Si substrate

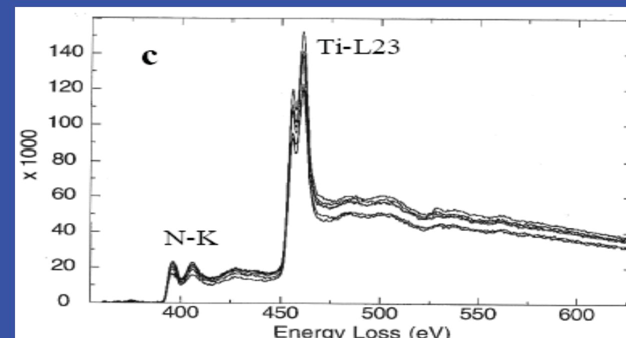

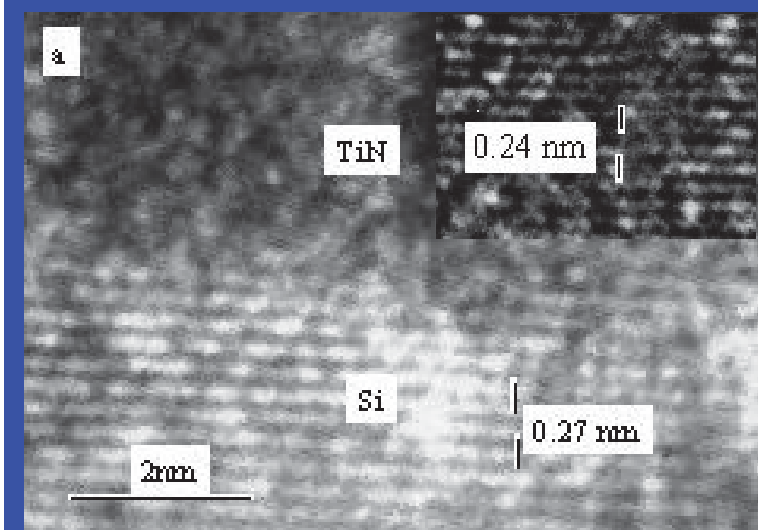

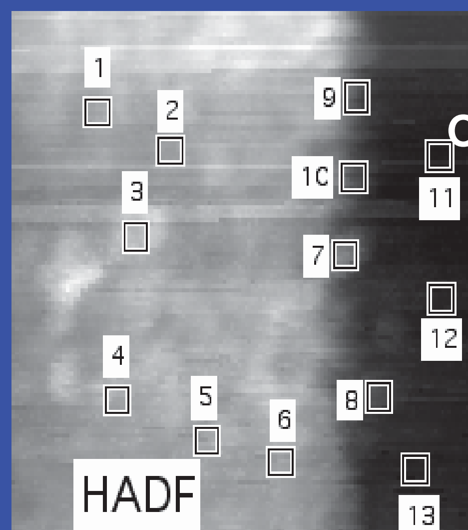

Spectrum analysis

On isolated clusters at the interface

at. conc. (± 10%)	Si	N	Ti	O
7	0.72	0.76	1	0.96
8	1	0.30	0.17	0.38

Dynamics of Polymorphic Nanostructures: From Growth to Collapse

F. Carlier,† S. Benrezzak,† Ph. Cahuzac,† N. Kebaïli,† A. Masson,† A. K. Srivastava,‡,§ C. Colliex,‡ and C. Bréchignac*,†

Laboratoire Aimé Cotton CNRS, Bât. 505, Université Paris-Sud, 91405 Orsay Cedex, France, and Laboratoire de Physique des Solides (UMR CNRS 8502), Bât. 510, Université Paris-Sud, 91405 Orsay Cedex, France

NANO LETTERS

2006
Vol. 6, No. 9
1875–1879

Received April 6, 2006; Revised Manuscript Received June 28, 2006

Impact Factor: 12.2

§ Permanent address: Division of Materials Characterization, National Physical Laboratory, Dr. K. S. Krishnan Road, New Delhi 110 012, India.

textile,
t thread
netic car-
innings,
process

Films from Clusters

In the "atom by atom" growth mode of inorganic films, strain induced by the substrate can largely control the final morphology, dictating outcomes ranging from a smooth film to island formation. Carlier *et al.* have explored the consequences of delivering material to a surface as clusters rather than individual atoms. Beams of antimony clusters were tuned to peak at different average sizes—either 88 atoms (Sb_{88}) or 300 atoms (Sb_{300})—and then directed toward a graphite surface. Both types of cluster formed fractal structures on this

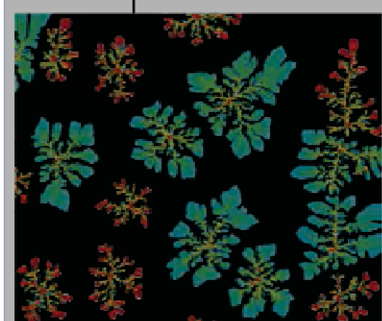

Sb_{88} clusters added to an Sb_{300} fractal network (yellow) produce initially compact end structures (red) that flatten after further deposition (cyan).

gas veloci-
ne convec-
observed
, consis-
onfigura-
gnetic

ing the initially thick end groups to flatten out and spread along the graphite in two dimensions. The authors suggest that this transition is triggered because the strain accumulating in the compact end groups eventually exceeds the surface energy cost of producing a flatter but more crystalline structure. — PDS

Nano Lett. 6, 1875 (2006).

13 OCTOBER 2006 VOL 314 SCIENCE

SCIENCE

Impact Factor: 31.4

EDITORS' CHOICE

EDITED BY GILBERT CHIN AND JAKE YESTON

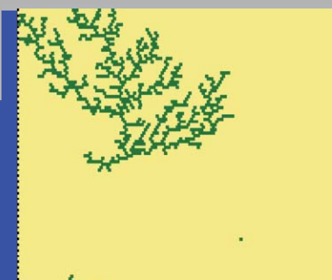

100 particles with 7 steps

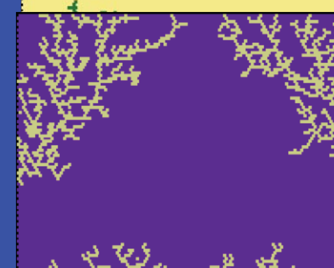

200 particles with 7 steps

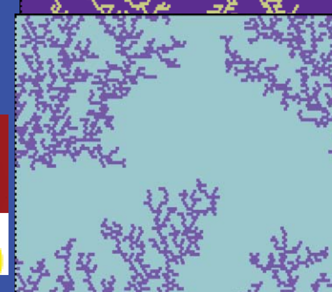

300 particles with 7 steps

Graphene – metal nanohybrid assemblies

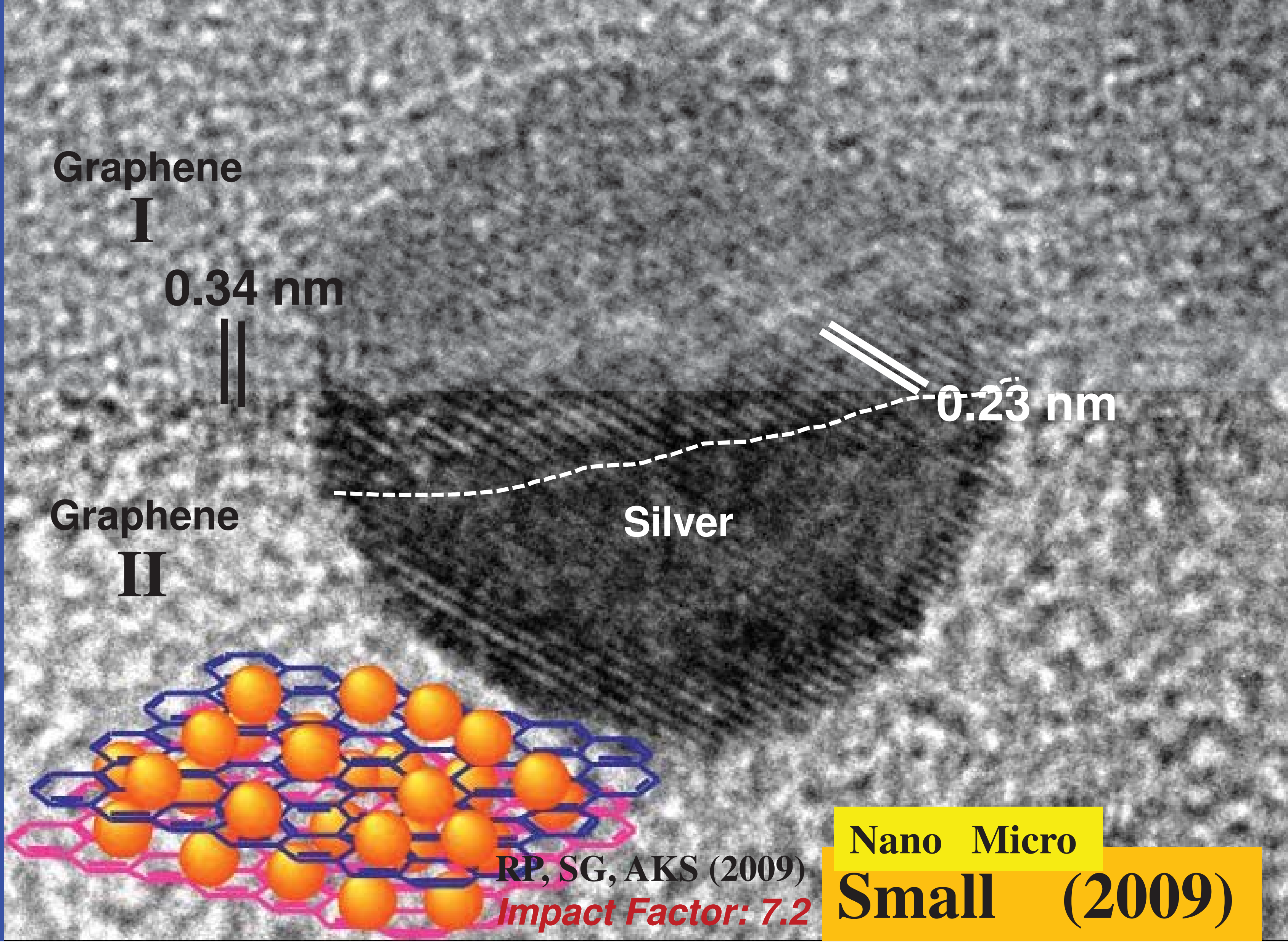

RP, SG, AKS (2009)
Impact Factor: 7.2

Nano Micro
Small (2009)

Scanning Helium Ion Microscope

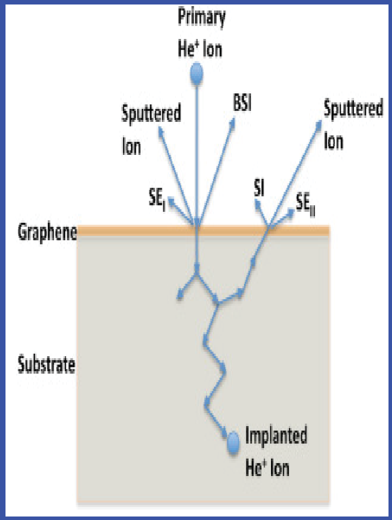

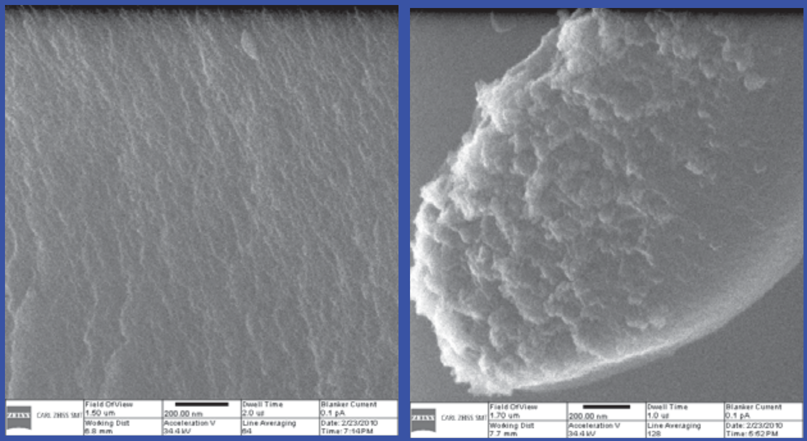

Morphological transformations from cellular to globular on individual nanoparticles of Al_2O_3

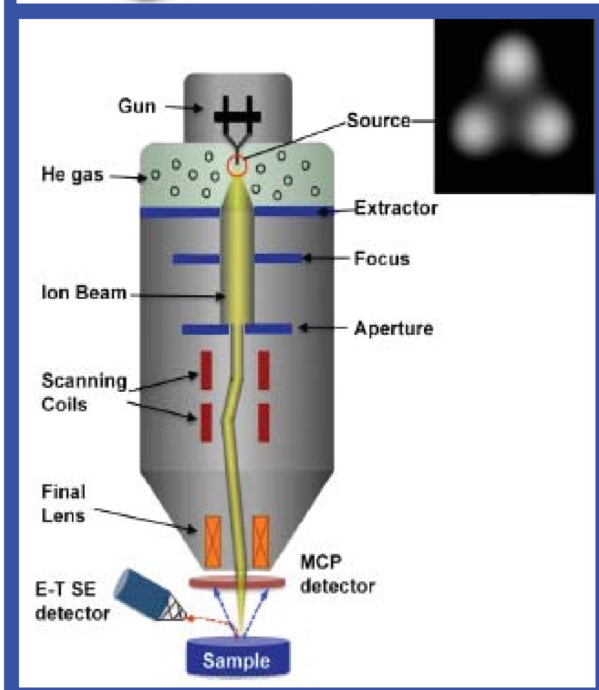

Schematic of helium ion microscope

राष्ट्रीय भौतिक प्रयोगशाला

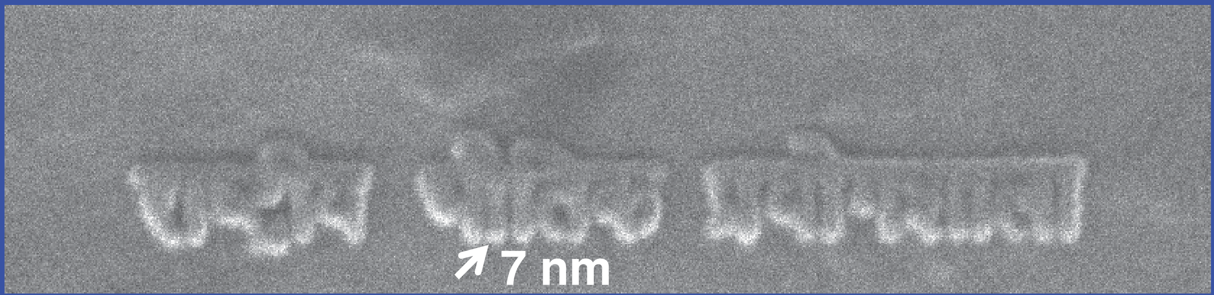

He ion microscopy showing nanopatterning by direct write deposition

Nano Scale Res Lett 2011

Toxic potential of materials at the nanolavel
(A.Nel, T.Xia, L.Madler and N.Li, Science, 311, 2006, 622)

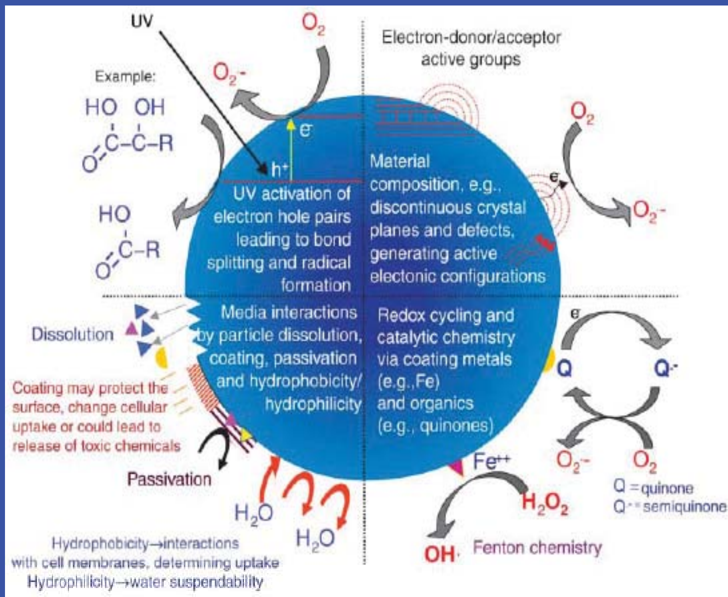

Possible mechanisms by which nanomaterials interact with biological tissue. Examples illustrate the importance of material composition, electronic structure, bonded surface species (e.g., metal-containing), surface coatings (active or passive), and solubility, including the contribution of surface species and coatings and interactions with other environmental factors (e.g., UV activation)

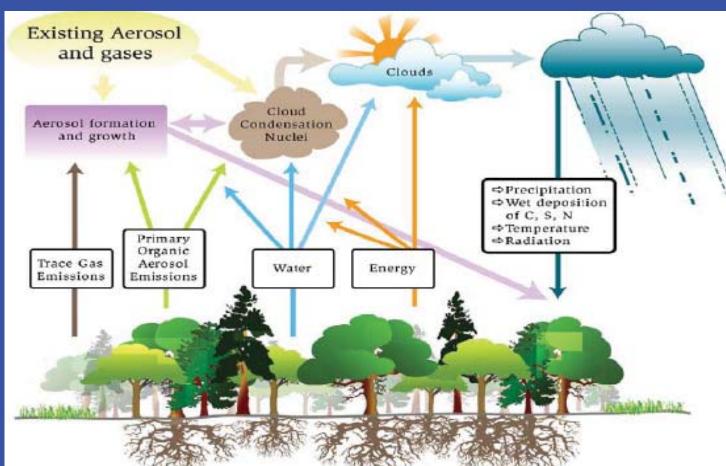

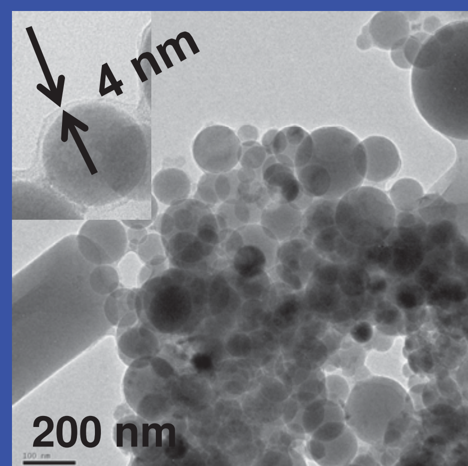

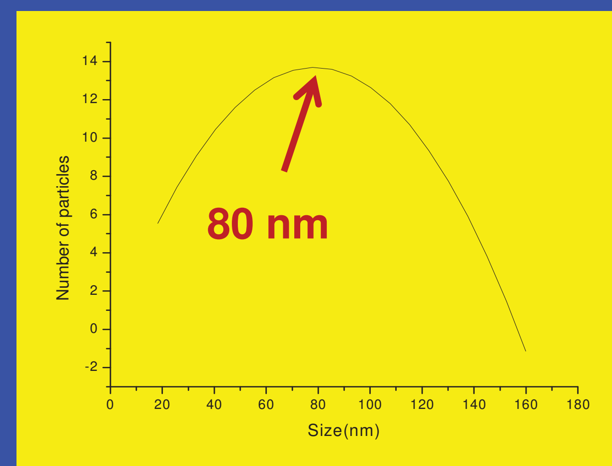

Schematic of the coupling of terrestrial ecosystems and the hydrologic cycle via energy and water exchange and aerosol processing (Barth et al Bull Amer. Meter. Soc. 2005)

Structure of the ISO TC229

Specific tasks include developing standards for: terminology and nomenclature; metrology and instrumentation, including specifications for reference materials; test methodologies; modeling and simulation; and science-based health, safety, and environmental practices.

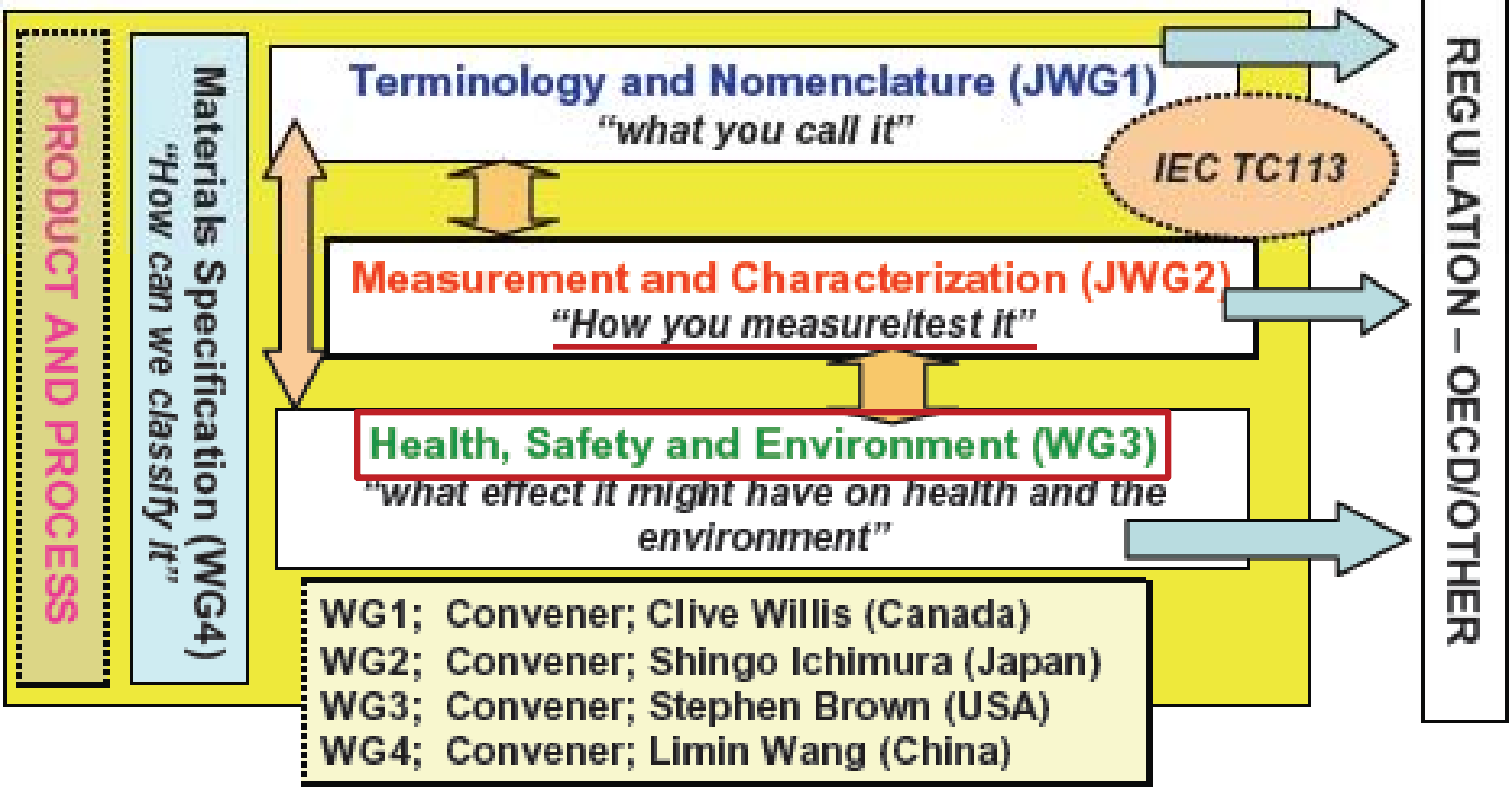

Opportunity from CHARGE

Detect deflections of electrons due to the presence of electric or magnetic fields, then we add electromagnetic information to the structural / crystallographic information

Electron wavefront modulation

Consider a magnetized particle: as electrons travel through, they are weakly deflected by magnetic field of particle. What was a plane wave, becomes a modulated wavefront

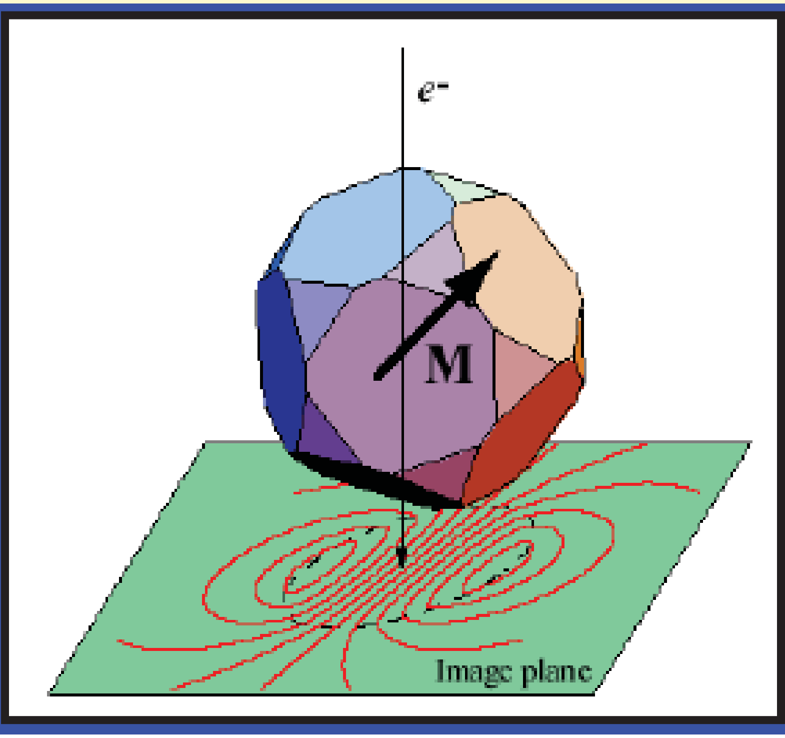

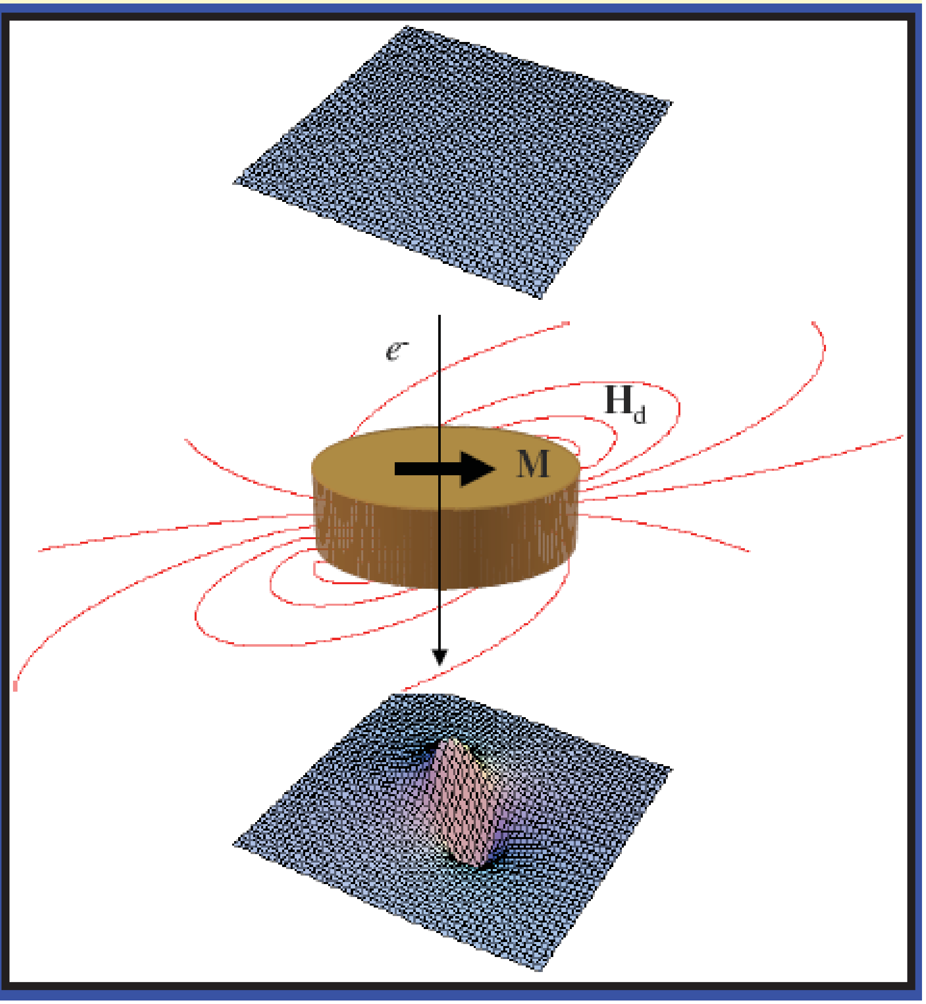

Magnetic domains in perovskite A_2FeMoO_6

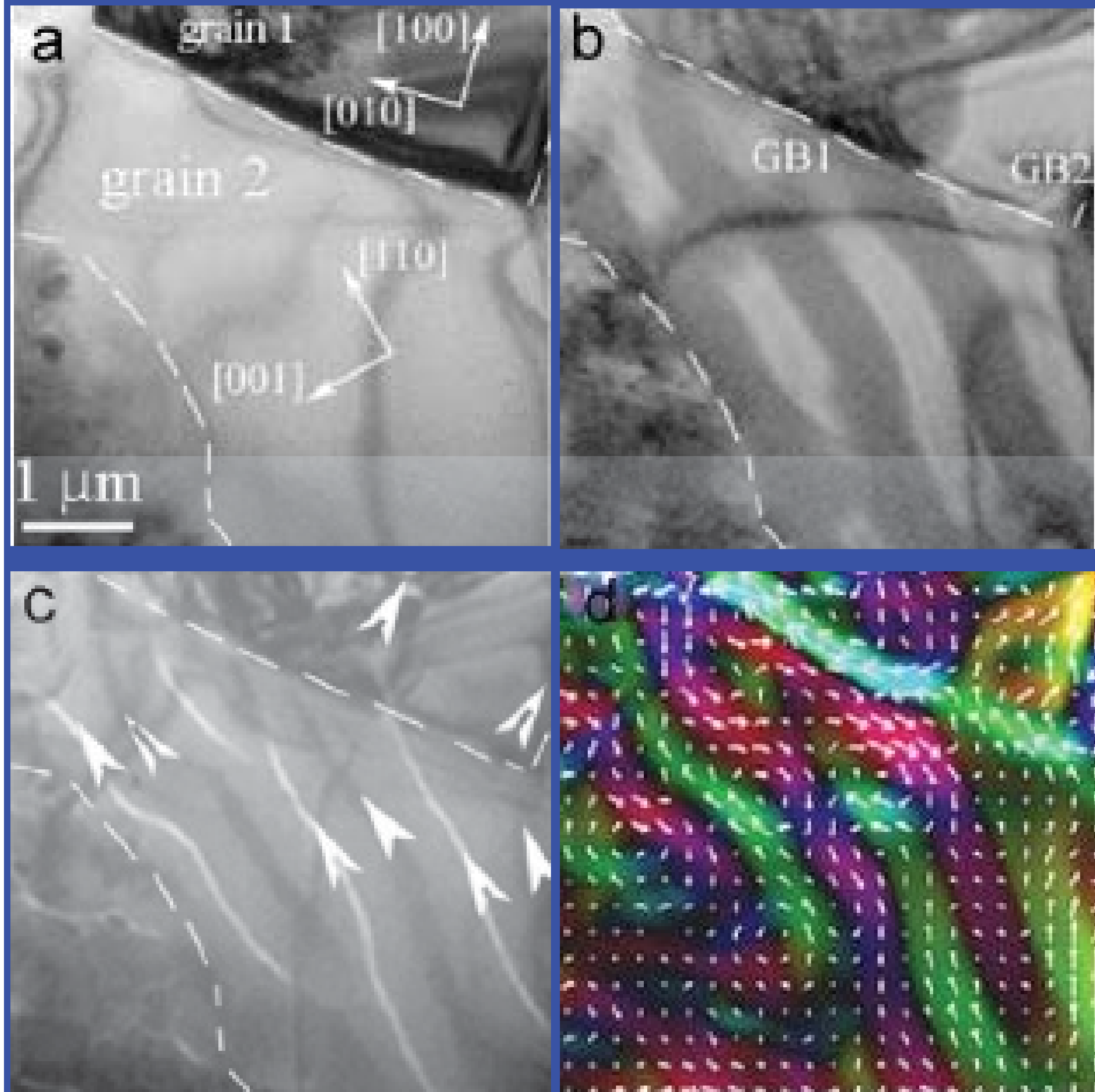

Lorentz TEM images of Ca_2FeMoO_6. (a) dark field image obtained by selecting the 002 spot. (b) Foucault image: white and black regions denote magnetic domains. © Fresnel image: white and black lines (indicated by white arrows) denote magnetic domain walls. Dashed lines in (a) – (c) are guides of grain boundaries. (d) The magnetization distribution obtained by the transport – of – intensity (TIE) method. The magnetizations are represented by white arrows. The TIE method was based on commercial software QPt with DM. Yu etal JMMM 2007

Most Important Recognitions / Achievements

Publications	Conferences	Chapters in Books	Invited lectures	Patent
140	105	04	45	01

Metallurgist of the Year – 2011, Ministry of Steel, Government of India

MRSI Medal – 2011 for contributions to the field of Materials Science and Engineering

Bharat Jyoti Award– 2011, India International Friendship Society

Kwan Im Thong Hood Award Travel Fellowship of Singapore

INSA – KOSEF Bilateral International Exchange Program fellowship 2009

BOYSCAST fellowship DST Government of India 2001, University of Paris

External Expert to Bureau of Indian Standards, Nanotechnology Program

Co-Chairman, Post Treatment Carbon Nanotubes, ICMAT 2011, Singapore

Establishment of High Resolution TEM Facility, Centre for Nanoscale Science at NPL

Visiting Scientist: UOP France, TUD Germany, UO Japan, POSTECH South Korea

High Resolution-TEM facility at NPL

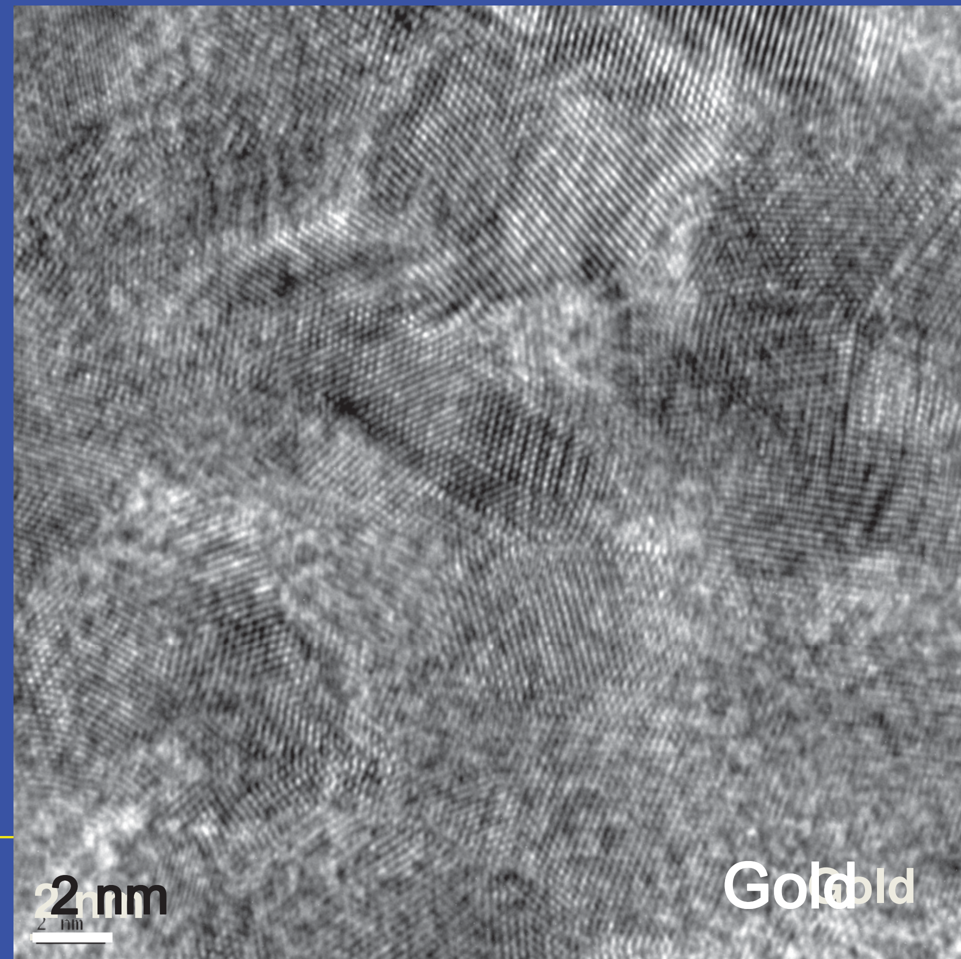

Important specifications and key features

TEM Point Resolution	: 0.205 nm
TEM Line Resolution	: 0.144 nm
STEM resolution	: 0.17 nm
EDAX resolution	: 136 eV

- *Fully integrated, optimized, easy-to-use interface*
- *Extensive applications-software support*

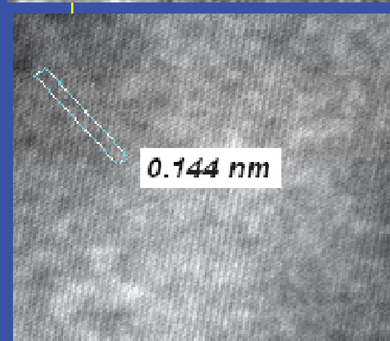

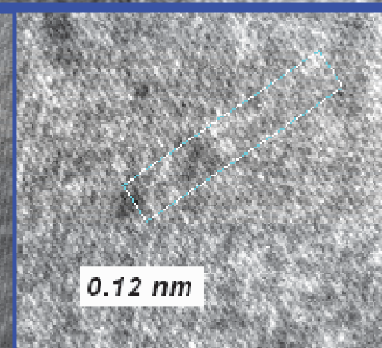

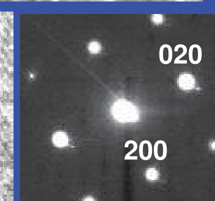

Ediffraction pattern; hkl: 200, 020 are markedlectron

Interplanar spacings: 0.144 nm 0.12 nm

Beam induced movement of gold atoms on surface
HR-TEM on TITAN with Image Cs-corrector @300kV

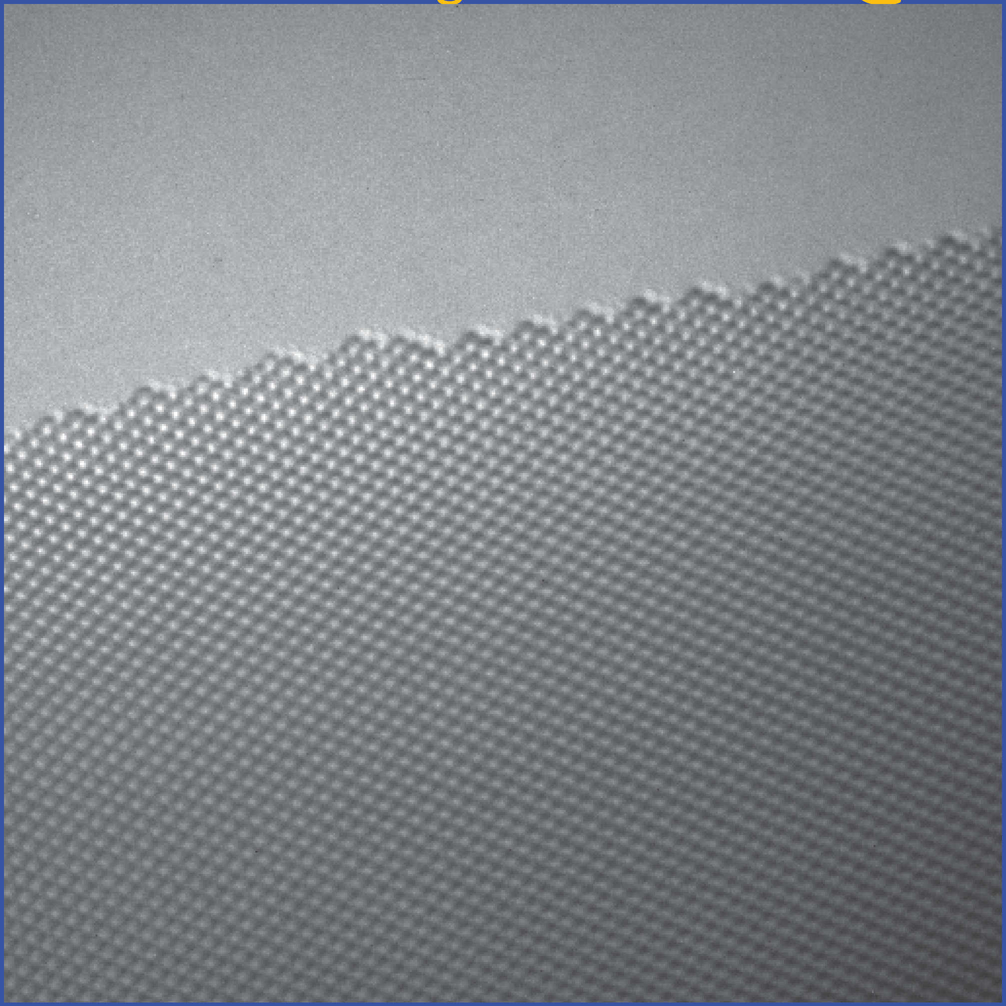

0.1nm

Image : B. Freitag , FEI

Movement of single atoms on surface can be monitored

Atoms are activated by focusing the beam maximal on the area

In situ growth of Pt crystals on Titan probe Cs-corrector

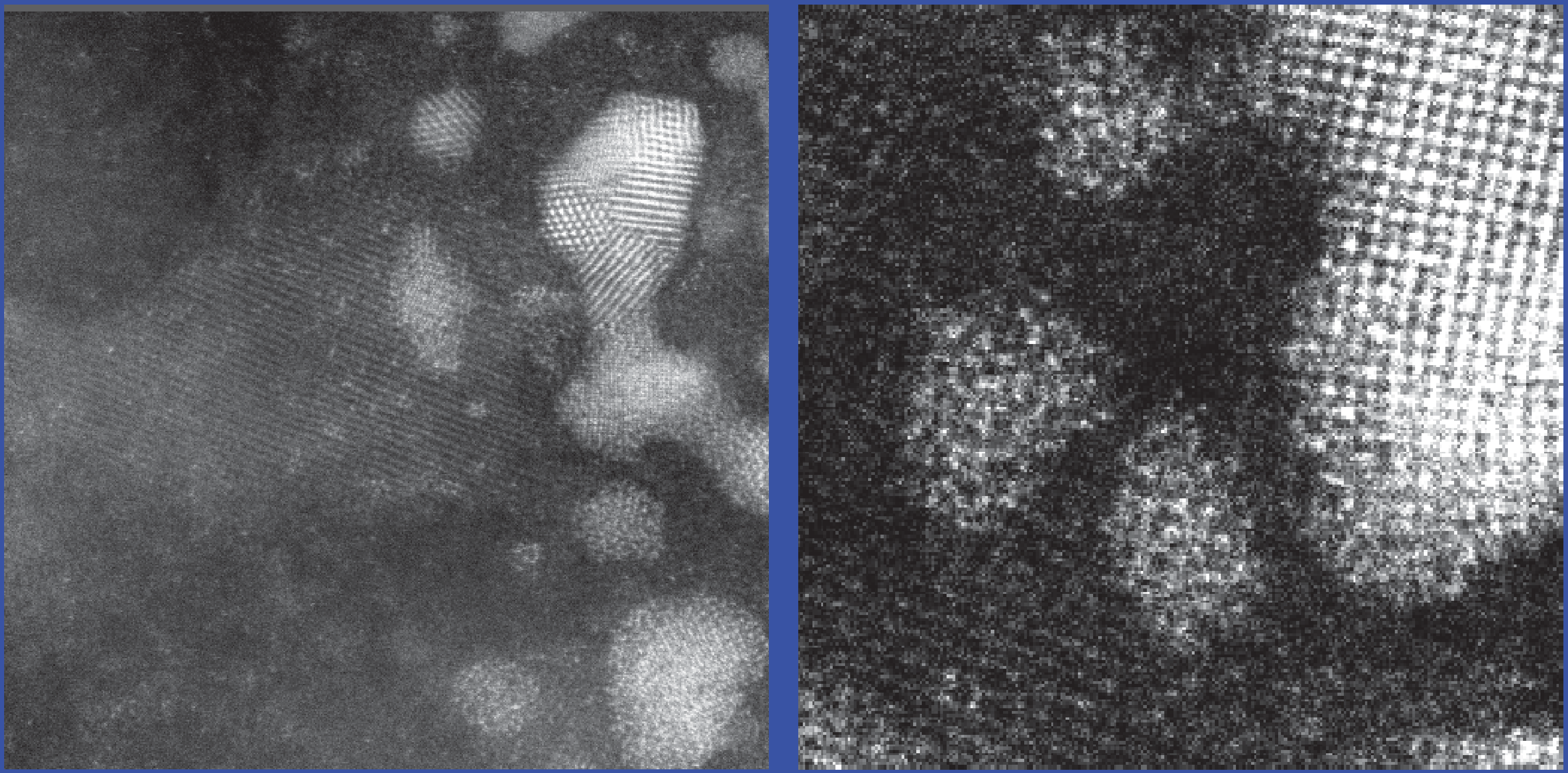

Beam induced growth of Pt clusters in Cs-corrected-STEM

The interaction of Pt clusters at the atomic level can be studied time resolved

Super Resolution Technology Map

SIM: Structured illumination microscopy; NSOM: Near field scanning optical microscopy; STED : Stimulated emission depletion microscopy; STROM : Stochastic optical reconstruction microscopy

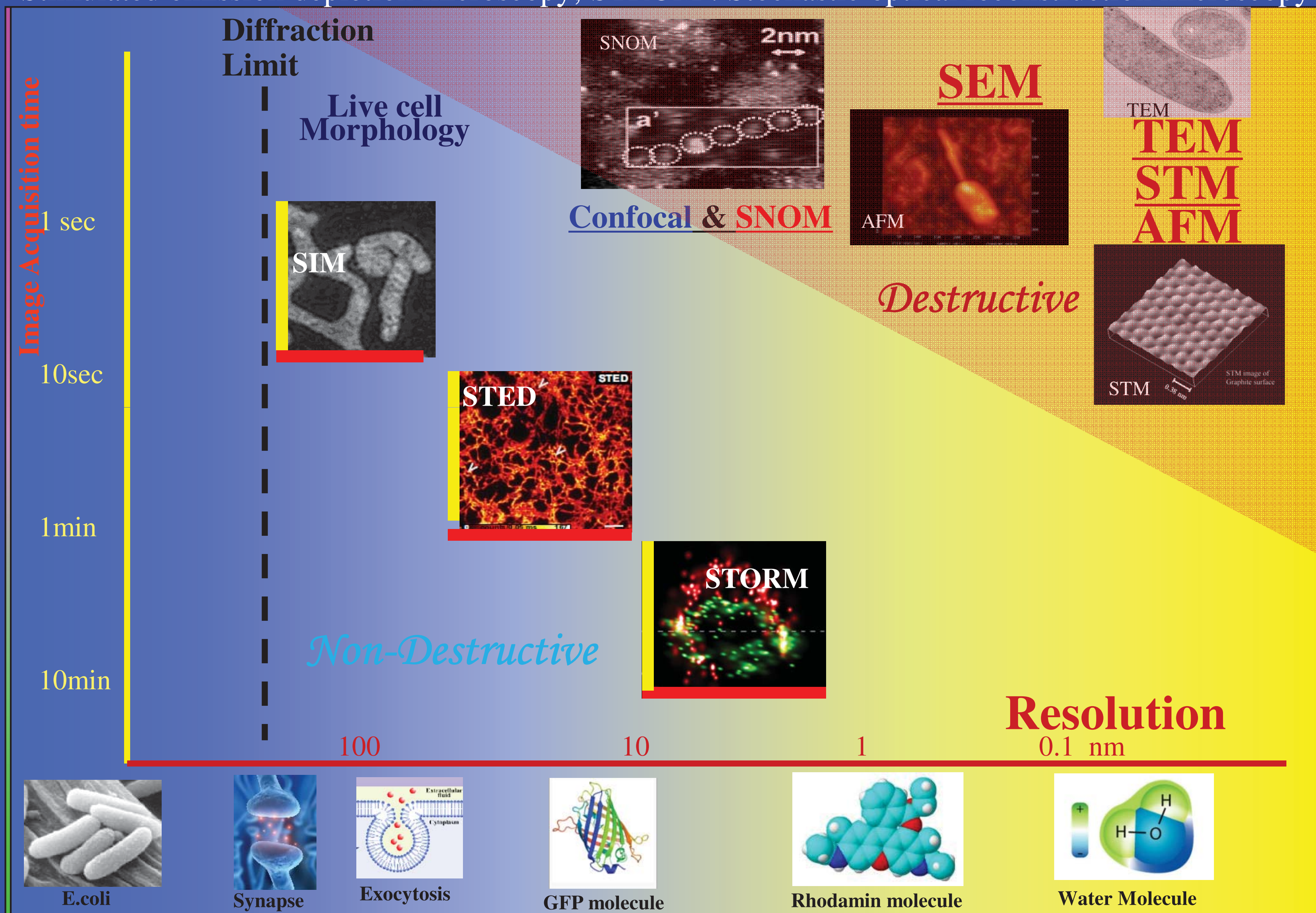

IMPORTANT REFERENCES / COLLABORATORS

Professor S. K. Joshi	I.I.T. Roorkee (UOR)	1986
Professor D. Chakravorty	I.I.T. Kanpur	1987
Professor T. R. Ramachandran	I.I.T. Kanpur	1988
Professor S. Ranganathan	I.I.Sc. Bangalore	1990
Professor K. Chattopadhyay	I.I.Sc. Bangalore	1990
Professor S. N. Ojha	I.T., B.H.U. Varanasi	1992
Professor E. S. Rajagopal	N. P. L. New Delhi	1996
Dr. Anil K. Gupta	N. P. L. New Delhi	1996
Professor Vikram Kumar	N. P. L. New Delhi	2003
Professor Sudhir Chandra	I. I. T. Delhi	2004
Professor R. C. Budhani	N. P. L. New Delhi	2009
Professor Christian Colliex	U.P.S. France	2001
Professor Kui Yu Zhang	U.O.R. France	2002
Professor H. A. Naseem	U.A.R.K. USA	2004
Prof. Dr. -Ing. h.c. Hartmut Fuess	T.U.D. Germany	2006
Professor Shin Toyoda	O.U.S. Japan	2007
Professor Kijung Yong	POSTECH Korea	2009
Professor Carlo S. Casari	NEMAS Italy	2009

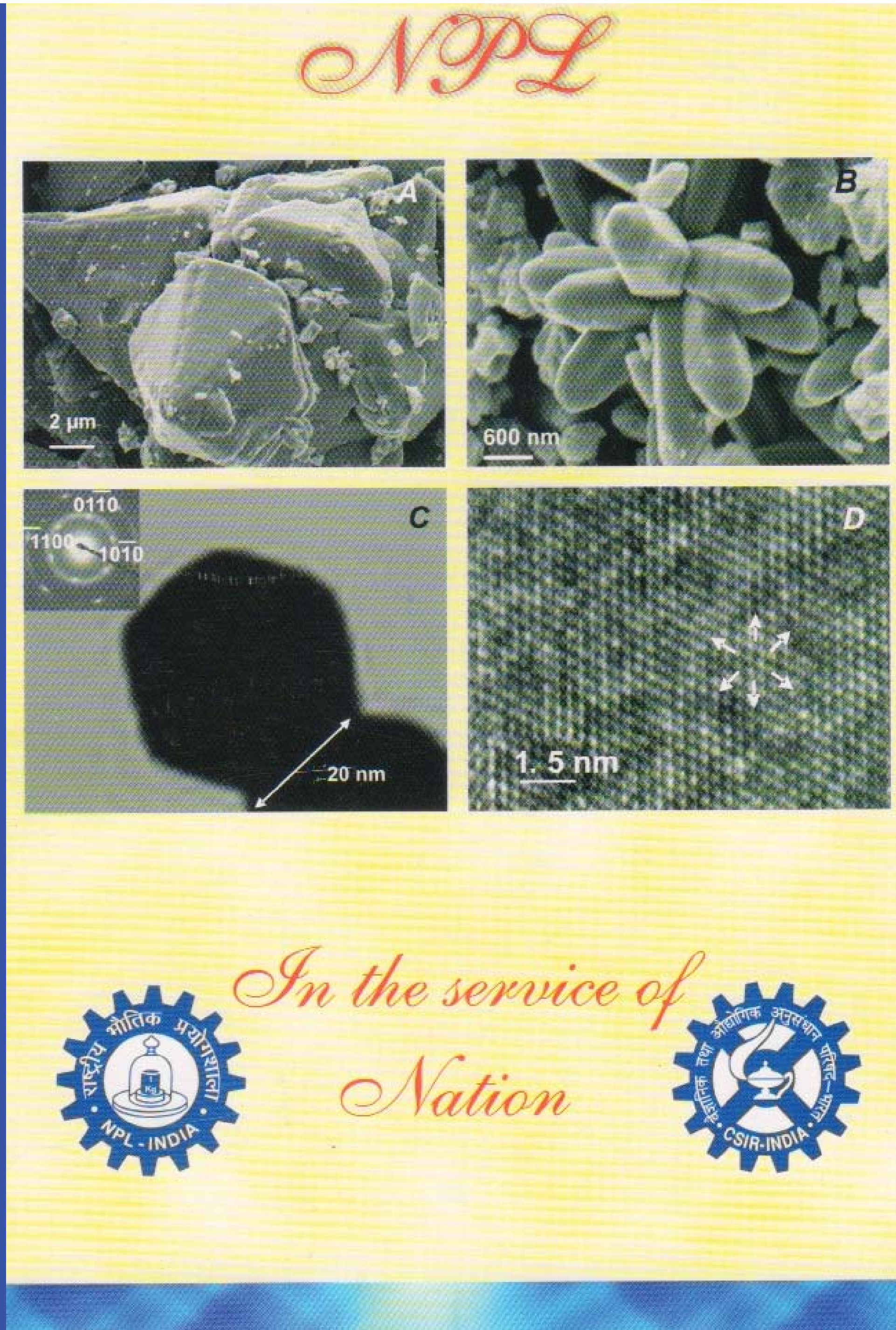

ZnO nanostructures on NPL new year greetings

Thank You